The Role of *Arabidopsis thaliana* P80 in Inositol Signaling

Padma Rangarajan

Thesis submitted to the faculty of the Virginia Polytechnic Institute and State University in partial fulfillment of the requirements for the degree of

Master of Science
In
Biochemistry

Glenda E. Gillaspy, Chair
Timothy J. Larson
Dorothea Tholl

8th May, 2013
Blacksburg, VA

Keywords: Inositol, P80, SnRK1, Signaling, HPLC, Inositol pyrophosphates, VIP kinases, *Arabidopsis thaliana*

The Role of *Arabidopsis thaliana* P80 in Inositol Signaling

Padma Rangarajan

ABSTRACT

The *myo*-inositol signaling pathway in plants allows them to sense external environmental stimuli and respond to them. This signaling pathway depends on the dynamic levels of the second messenger, inositol(1,4,5)trisphosphate, which in turn is regulated by inositol polyphosphate 5-phosphatases (5PTases). Previous studies have shown that 5PTase 13 binds an important energy sensor, Sucrose non-fermenting (Snf) 1-related kinase (SnRK1.1) and also a novel protein P80. Studies from the lab have also shown that P80 is a part of a deubiquitinating enzyme complex along with WDR20 and Ubiquitin-specific protease called UBP3. Our *p80* mutants have a root deficient phenotype under low energy conditions which is normalized by addition of sucrose. *p80* mutants show reduced growth and early senescence under specific environmental conditions. This is opposite in nature to SnRK1.1 overexpressors. In this study, I have examined the possible interaction of P80 with SnRK1. I have studied the effects of expression of the exogenous SnRK1.1:GFP transgene under the control of the 35S CaMV promoter in the *p80* mutant. This will facilitate the delineation of mechanisms that plants use for the control of energy sensing. I also examined the effects of the overexpression of SnRK1.2:GFP in the *p80* mutant. Further, I have explored the presence of a new class of molecules, inositol phosphate molecules (InsPs) containing pyrophosphate bonds (PPx) in *p80* mutants. Recent evidence has shown that this class of molecules has roles in sensing and signaling. I have demonstrated that $InsP_7$ is present in developing seeds and vegetative tissue of higher plants. I have also demonstrated that *p80* mutants have an alteration in the levels of PPx-InsPs. In addition, I have established spatial expression patterns of two enzymes involved in the synthesis of PPx-InsPx, known as VIP kinases. These studies will help resolve how PPx-InsPs are regulated in plants and thus help in their functional characterization.

ACKNOWLEDGEMENTS

First and foremost, I would like to thank my advisor, Dr. Glenda Gillaspy. I am extremely grateful to her for being a wonderful mentor throughout my tenure as a graduate student. She has been there for me whenever I needed her, as a supportive and encouraging guide. I will always cherish the opportunity that she provided me to grow as a researcher and develop as a better individual.

I want to thank Janet Donahue, our lab technician, for teaching me so many techniques in the lab methodically and answering each of my questions patiently. I also want to thank my lab mate and close friend, Phoebe Williams for being a great coworker to talk science with. I want to take this opportunity to thank Mihir Mandal, our post doc for giving me lots of feedback on my research and Juin Yen, another lab member for providing a friendly work environment. I would like to thank my committee members Dr. Timothy Larson and Dr. Dorothea Tholl for their assistance in my research.

TABLE OF CONTENTS

LIST OF FIGURES

CHAPTER I

CHAPTER II

CHAPTER III

CHAPTER IV

LIST OF TABLES

LIST OF ABBREVIATIONS

5PTase	*myo*-inositol polyphosphate 5-phosphatase
AMPK	AMP-activated protein kinase
DDP	diphosphoinositol polyphosphate phosphohydrolase
DUB	deubiquitinating enzymes
FANCD2	Fanconi anemia, complementation group D2
GFP	green fluorescent protein
GRIK	geminivirus Rep-interacting kinase
GUS	β-glucoronidase
HPLC	high pressure liquid chromatography
Ins	*myo*-inositol
InsP	Inositol phosphate
Ins(1,4,5)P_3	*myo*-inositol-(1,4,5)triphosphate
InsP_6	inositol hexakisphosphate
InsP_7	diphosphoinositol pentakisphosphate
InsP_8	bisdiphosphoinositol tetrakisphosphate
MS	Murashige and Skoog
P80	Arabidopsis protein of 84 kDa size
PLC	phospholipase C
PHLPP	PH domain and Leucine rich repeat Protein Phosphatases
PPx-InsPs	diphosphorylinositol polyphosphates
PtdIns	phosphatidylinositol
PtdIns(4,5)P_2	phosphatidylinositol(4,5)bisphosphate
qRT-PCR	quantitative real-time polymerase chain reaction

Snf1	sucrose non-fermenting 1
SnRK1	snf-related kinase 1
UAF1	ubiquitin specific-protease1 Activating Factor1
USP	ubiquitin specific protease
WD	tryptophan-aspartic acid dipeptide
WDR20	WD40-repeat containing protein
WT	wild-type

CHAPTER I

INTRODUCTION

One of the most important abilities of living organisms is survival. Plants, owing to their sessile nature, have adopted several strategies essential for survival. These strategies include nutrient sensing from the environment and responses to various stimuli (Liu et al. 2009). The exploration of the mechanism and regulation of these strategies will help elucidate novel ways to increase plant survival, growth and development (Baena-Gonzalez et al. 2007).

myo-inositol (Ins) is a simple polyol that can, with addition of lipids or phosphates, result in the production of second messengers (Gillaspy 2011). In plants, the Ins signaling pathway is essential in the response to the environment (Michell, 2007). This signal transduction pathway has been shown to be involved in the way plants respond to environmental stimuli like gravity (Perera et al. 2006), light (Chen et al. 2008) and water (Munnik et al. 2010) ; recent data connects this pathway to energy sensing (Ananieva et al. 2008).

The Ins signaling pathway begins with a signal like nutrient stress or light availability that triggers the activity of phospholipase C (PLC), thus generating inositol(1,4,5)triphosphate ($InsP_3$) from phosphatidylinositol(4,5)bisphosphate [PtdIns(4,5) P_2]. In animals, $InsP_3$ binds to intracellular receptors that function to release Ca^{2+} from intracellular stores, initiating downstream biological processes. However, in plants, a Ca^{2+} receptor has not been identified, hence the possibility of a unique Ca^{2+} release mechanism has been debated (Krinke et al. 2007). $InsP_3$ is hydrolyzed to inositol(1,4)bisphosphate [Ins(1,4)P_2] by a group of enzymes called *myo*-inositol polyphosphate 5-phosphatases (5PTases), resulting in the decrease of intracellular Ca^{2+} and termination of signal transduction (Munnik et al. 1998; Gillaspy 2011). Ins(1,4) P_2 can be then converted to Ins by the sequential action of two more Ins phosphatases (Figure 1).

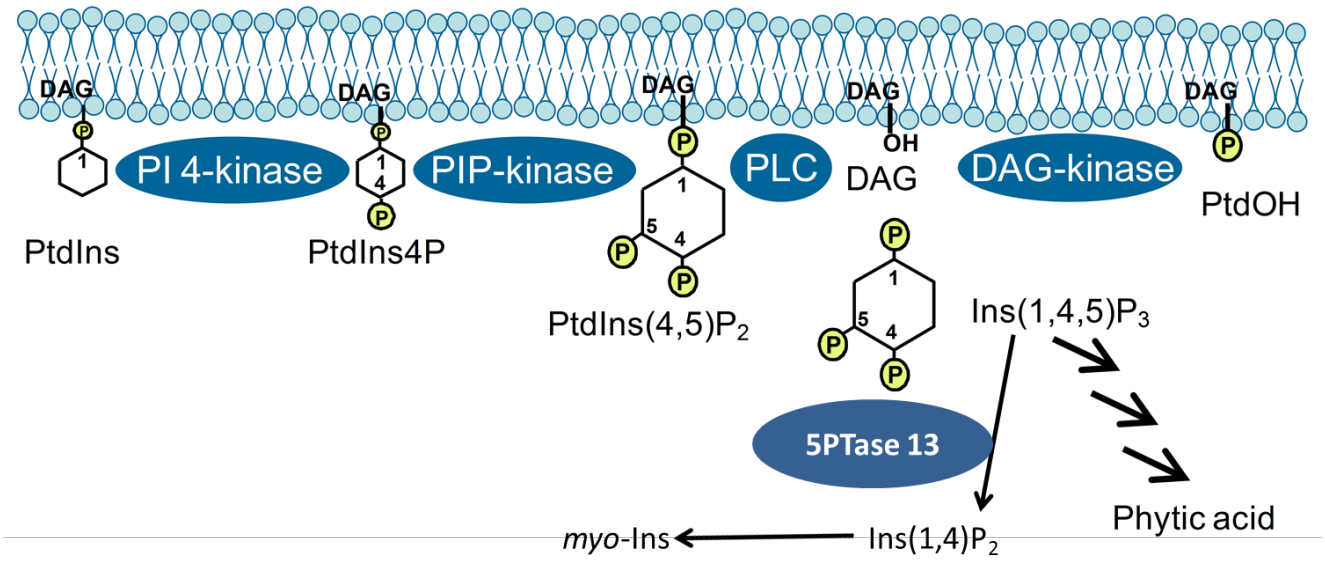

Figure 1: An Overview of Inositol Signaling.

This figure has been reprinted with modifications with permission from the author, Ingo Heilmann. The Ins Signaling pathway begins with a signal, triggering the activity of Phospholipase C (PLC). PLC breaks down PtdIns(4,5)P_2 to form $InsP_3$ and DAG. In animals, $InsP_3$ binds to intracellular receptors that function to release Ca^{2+} from intracellular stores, resulting in downstream biological responses. $InsP_3$ can be phosphorylated to form phytic acid. $InsP_3$ is then hydrolyzed to $InsP_2$ by a set of enzymes called 5PTases. $InsP_2$ is then converted to inositol by enzymes known as Inositol monophosphatases or IMPs.

LITERATURE REVIEW

The Role of 5PTases in Inositol Signaling

Like many eukaryotes, plants regulate the amount of the molecule $InsP_3$ using 5PTases. These enzymes have been have been widely studied in *Arabidopsis thaliana* (Gunesekera et al. 2007; Ercetin et al. 2008; Wang et al. 2009; Kaye et al. 2011).

The Arabidopsis genome contains fifteen genes that encode fifteen different 5PTase proteins (Berdy et al. 2001). These vary in size and have been categorized as Group I (5PTase 1-11) and Group II (5PTase 12-15). Group I consists of smaller proteins that are related to the 5PTases from other organisms. The second group, Group II contain unique N-terminal WD repeats in addition to a 5PTase catalytic domain (Zhong et al. 2004). The name 'WD40' stems from the conserved amino acids Tryptophan and Aspartic acid dipeptide found at the end of a 40 amino acid protein sequence (Smith et al. 1999). Structurally, these WD dipeptides occur several times in a protein and together known to adopt a β-propeller conformation. WD40 repeats usually facilitate protein-protein interactions and have been implicated in various different cellular functions, namely, cell cycle control, pre-mRNA processing, signal transduction and histone recognition (Smith et al. 1999; Li et al. 2001).

5PTases have been found to play a number of roles in plant growth and development. Gunasekera et al. (2007) found *At*5PTase1 and 5PTase2 play a role in seed germination and development. They also showed that seedlings with mutations in those genes displayed higher levels of $InsP_3$ and lower levels of PtdIns, PtdIns(4)P, and PtdIns(4,5)P_2. Other work has elucidated the roles of 5PTases in root gravitropism (Wang et al. 2009), regulation of production of reactive oxygen species, salt tolerance (Kaye et al. 2011) and seedling growth (Ercetin et al. 2008). 5PTases have also been determined to play a role in auxin homeostasis (Lin et al. 2005) and light signaling (Chen et al. 2008). 5PTases are important for several aspects of plant development; a better understanding of these enzymes will help to explore the ways in which plants respond to environmental signals.

The Role of Sucrose Non-Fermenting Kinases (SnRKs) in the Ins Signaling Pathway

One specific 5PTase from *Arabidopsis* called 5PTase13 has been found to associate with the known energy sensor named sucrose non-fermenting-1 (*snf-1*)- related kinase 1 (SnRK1.1). 5PTase 13 contains five WD40 repeats in its N-Terminus, along with a conserved 5PTase domain. To investigate the WD40 regions and their ability to participate in protein complexes, 533 N-terminal amino acids containing the WD40 repeats were used as bait in a yeast two-hybrid screen. A positive clone containing the C-terminal domain of SnRK1.1 gene was obtained from the screen. It was also concluded that 5PTase13 and SnRK1.1 could form a protein complex *in vitro* (Ananieva et al. 2008). Furthermore, SnRK1.1 activity was found to be altered in the *5PTase13* mutants and varied with nutrient conditions. It was concluded that 5PTase 13 stabilized SnRK1.1 under low nutrient conditions (Ananieva et al. 2008).

SnRK1.1 is a member of a small gene family in plants, and is considered to be the paralogue of the Adenosine Monophosphate Activating Kinase (AMPK), a low energy sensor and master regulator of metabolism in animals (Hardie 2011). AMPK is activated during low ATP conditions, and in turn phosphorylates substrate proteins resulting in suppression of anabolic pathways and stimulation of catabolic pathways (Hardie 2011). AMPK stimulates several essential functions such as glucose absorption, homeostasis, cell growth and development (Hardie 2008; Hardie 2011). The yeast paralogue of AMPK, called Snf1 (Sucrose Non-Fermenting Kinase 1), also functions to regulate metabolism in response to glucose (Hardie 2007). SnRK1.1 from Arabidopsis was found to complement the *snf1* mutation in yeast (Alderson et al. 1991), indicating SnRK1.1 may play a similar role in Arabidopsis.

In plants, there is a large group of SnRK family proteins and these have been phylogenetically classified as SnRK1, SnRK2 or SnRK3 sub-family members. All function as serine-threonine kinases (Halford 2009). These three groups of SnRKs are considered to act on different substrates. Work has shown that SnRK2 and SnRK3 cannot compensate for the loss of SnRK1 (Zhang et al. 2001; McKibbin et al. 2006). However recently, the possibility of the SnRKs having a connected role, and even have similar substrates was demonstrated by Zhang et al (Zhang et al. 2008). For my work it is important to note that even though several SnRK

proteins have been found to play a role in plant signaling, SnRK1 proteins are the accepted plant paralogues of the AMPK, and these have been documented to play a unique role in nutrient and stress signaling (Baena-Gonzalez et al. 2007).

SnRK1.1 plays a role in metabolism and signaling

There are three SnRK1 genes in Arabidopsis, *SnRK1.1*, *SnRK1.2* and *SnRK1.3*. A CLUSTALW alignment of the encoded SnRK1 proteins is shown in Figure 2. *SnRK1.3* is widely believed to be a pseudogene and data suggest that this gene is not expressed under any conditions in plants (Baena-Gonzalez et al. 2007). SnRK1.1 and SnRK1.2 each have three splice variants, that may produce different proteins (SnRK1.1.1, SnRK1.1.2, SnRK1.1.3 and SnRK1.2.1, SnRK1.2.2, SnRK1.2.3). All three splice variants of SnRK1.1 encode a protein kinase, Kinase associated (KA1) and Ubiquitin Associated (UBA) domains. SnRK1.1.2 differs from SnRK1.1.1 and SnRK1.1.3 in that a 23 amino acid (AA) N-terminal extension is present in the encoded protein. The function of this 23 AA is not known, but it is intriguing and reasonable to speculate that it is involved in subcellular location. SnRK1.1.1 may differ in its 3'UTR sequence resulting in a novel 81 AA extension at the C-terminus. However the cDNA clone used to make this prediction may contain a sequencing error and the Arabidopsis Information Resource (TAIR) has predicted only two discrete SnRK1 proteins to exist. One splice variant of SnRK1.2 does encode the KA1 domain, but the other two are predicted to encode proteins very structurally similar to SnRK1.1. The role of SnRK1.2 in energy sensing is yet unclear. Data suggest that the functional role of SnRK1.2 may be redundant with SnRK1.1 (Baena-Gonzalez et al. 2007) while unpublished data from the Gillaspy lab indicates that SnRK1.2 has a unique, restricted expression pattern (in lateral roots and apical meristems).

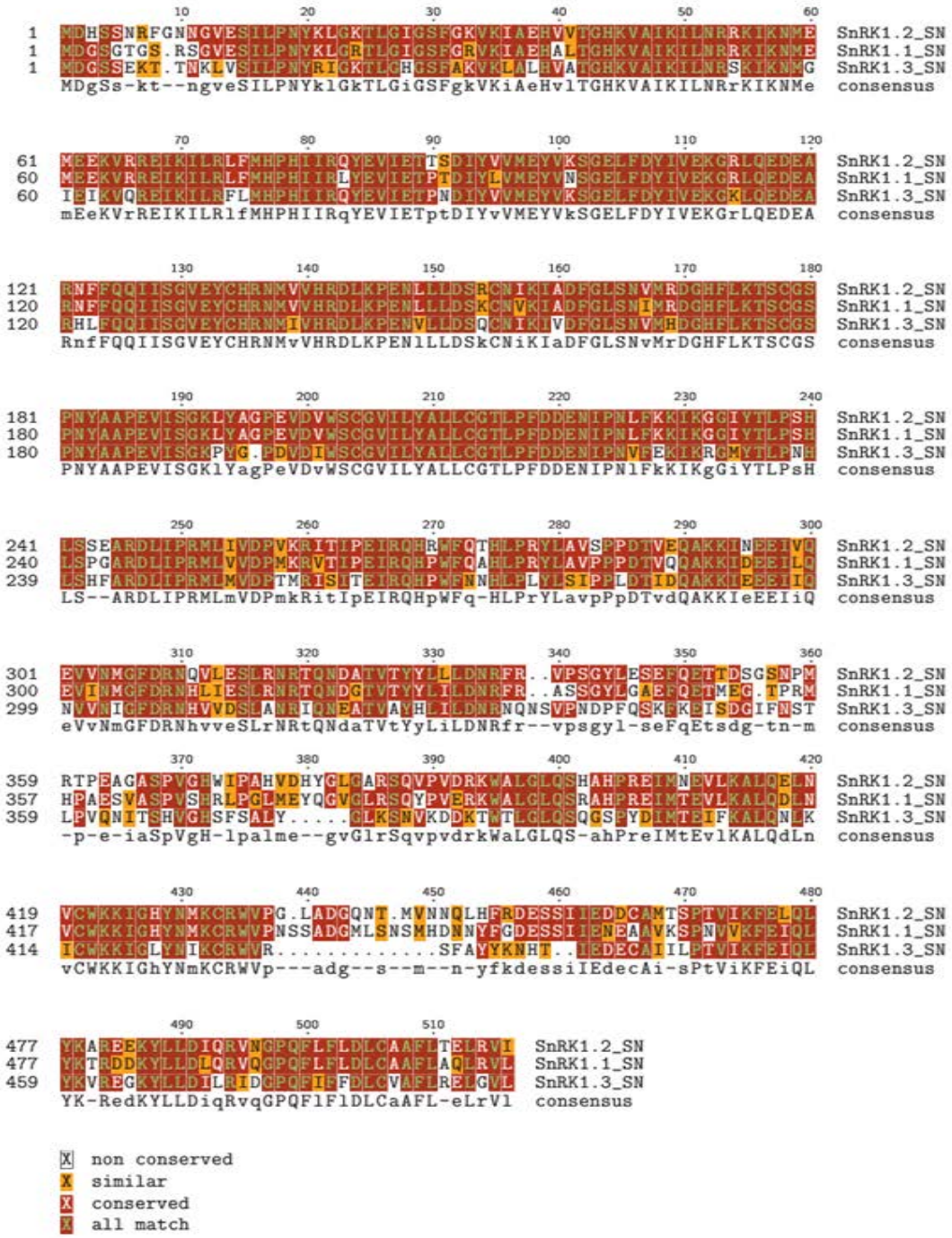

Figure 2: Alignment of SnRK1 Proteins.

CLUSTALW was used to align all predicted SnRK1 proteins. Analysis shows that SnRK1.1 and SnRK1.2 share 80% homology, while SnRK1.1 and SnRK1.3 share 67% homology. SnRK1.2 and SnRK1.3 protein sequences are predicted to be 69% homologous.

Regulation of SnRK

The AMPK/SnRK1 protein kinases function as heterotrimeric complexes. These complexes consist of a catalytic α-subunit (encoded by the SnRK1.1 and SnRK1.2 genes) and β and γ subunits for protein stability and kinase activities (Ghillebert et al. 2011). However, plants also display alternate plant-specific complexes besides the typical heterotrimeric complex (Slocombe et al. 2002). Phosphorylation of the catalytic subunit is required for AMPK/SnRK1 activation. Sequence comparison with the kinases activating the mammalian AMPK and yeast SNF1, along with complementation and phosphorylation assays have implicated Geminivirus Rep-interacting kinase 1/2, also known as GRIK1/2 or SnAK1/2 as the upstream activating kinases of SnRK1 in plants (Shen et al. 2009). The GRIK proteins have been found to bind to SnRK1.1 and SnRK1.2 and phosphorylate specific threonine residues in the activation loop. This phosphorylation results in an increase in the SnRK1 kinase activity (Shen et al. 2009). PP2A and PP2C phosphatases have been reported to dephosphorylate and then inactivate mammalian AMPK and plant SnRK1 *in vitro*, however specific phosphatases that are involved in the inactivation *in vivo* have not yet been identified (Sugden et al. 1999).

A Potential Regulator of SnRK1.1 called Protein 80 (P80)

As mentioned, studies from the Gillaspy lab have shown that SnRK1.1 is a binding partner of 5PTase 13, and that 5PTase13 expression in seedlings under low energy conditions is associated with stabilization of SnRK1.1. Dr. Les Erickson, our collaborator, also identified the gene (At3g05090) encoding a protein named P80 in yeast two hybrid assays using the 5PTase13 WD40 repeats as bait. A former graduate student in the lab determined that 5PTase13 and P80 recombinant proteins associate *in vitro*, but the P80/SnRK1.1 interaction was weak. Dr. Erickson has subsequently examined P80/SnRK1.1 interactions in yeast, and found there is no interaction. Thus, P80 may not associate directly with SnRK1.1 (Figure 3).

The Arabidopsis *P80* open reading frame encodes a 753 amino acid protein with a predicted molecular weight of about 84 kDa. Analysis of conserved domains reveals six WD40 repeats in the N-terminus of P80. There may be a seventh WD40 repeat in the amino acids, 435-441. A Phyre2 predicted model of the protein is depicted in Figure 4 (Kelley L.A 2009). Phyre2 uses the alignment of hidden Markov models and folding simulation called Poing to model regions of a protein of interest to a three dimensional structure.

The homolog of P80 in humans is the Ubiquitin specific-protease1 Activating Factor 1 (UAF1) (Figure 5). Human UAF1 forms part of a Deubiquitinating enzyme (DUB) complex. Deubiquitination is the process of the removal of ubiquitin molecules. UAF1 regulates the activity of different enzyme complexes involving three different DUBs, USP1, USP12 and USP46 (Cohn et al. 2009; Kee et al. 2010). The DUB complex of USP12-UAF1 also requires the activity of another protein, a WD40-repeat containing protein named WDR20 (Kee et al. 2010).

The human UAF1 contains 677 amino acids, including seven to eight WD40 repeats in the N-terminal half and a predicted coiled-coil domain in the C-terminal half (Park et al. 2002; Cohn et al. 2007). Structure prediction using Phyre2 predicts UAF1 has a propeller structure comprising of the WD40 repeats (Cohn et al. 2007). It has an approximate mass of 80 kDa.

The DUB complex, USP1/UAF1 plays an important role in the Fanconi anemia pathway (Nijman et al. 2005). The Fanconi anemia pathway in humans is involved in repairing DNA crosslinks. A key step in this pathway involves mono-ubiquitination of Fanconi anemia

complementation group D2 (FANCD2) protein within the nucleus. Deubiquitination of the FANCD2 protein by the USP1/UAF1 complex is essential for an intact Fanconi anemia pathway. Inefficient deubiquitination of the FANCD2 protein within the nucleus, leads to an accumulation of monoubiquitinated FANCD2, resulting in the dysregulation of the pathway and hypersensitivity to DNA cross-linking agents (Nijman et al. 2005). Human USP1 also plays an important role in DNA damage response and cancer-related processes (Garcia-Santisteban et al. 2012). The USP12/UAF1 complex is involved in the regulation of the Notch signaling pathway in animals (Moretti et al. 2012). The USP46/UAF1 complex is involved in the regulation of PH domain and Leucine rich repeat Protein Phosphatases (PHLPP), which is an enzyme that functions as a tumor suppressor in the Protein Kinase B or AKT signaling pathway(Imai et al. 2013).

Studies from the Gillaspy lab have shown that P80 is also part of a DUB complex along with two other proteins, the plant homolog of the WD40-repeat containing protein, WDR20 (At2g37160) and USP46 paralogue in plants called UBP3 (At4g39910). WDR20 in humans serves as a stimulatory subunit of the UAF1/USP complexes (Kee et al. 2010). However, the role of this protein in plants is yet to be elucidated. UBP3 in Arabidopsis has been shown to be involved in pollen development. The deubiquitination of one or more targets by UBP3-containing DUB complex may be required for the development of functional pollen (Doelling et al. 2007). It is reasonable to hypothesize that P80, along with UBP3 and WDR20 may be involved in the deubiquitination of different target proteins. Given the significance of its human homolog, the Arabidopsis P80 stands out as an important protein which may be essential for the proper growth, development and functioning of the plant.

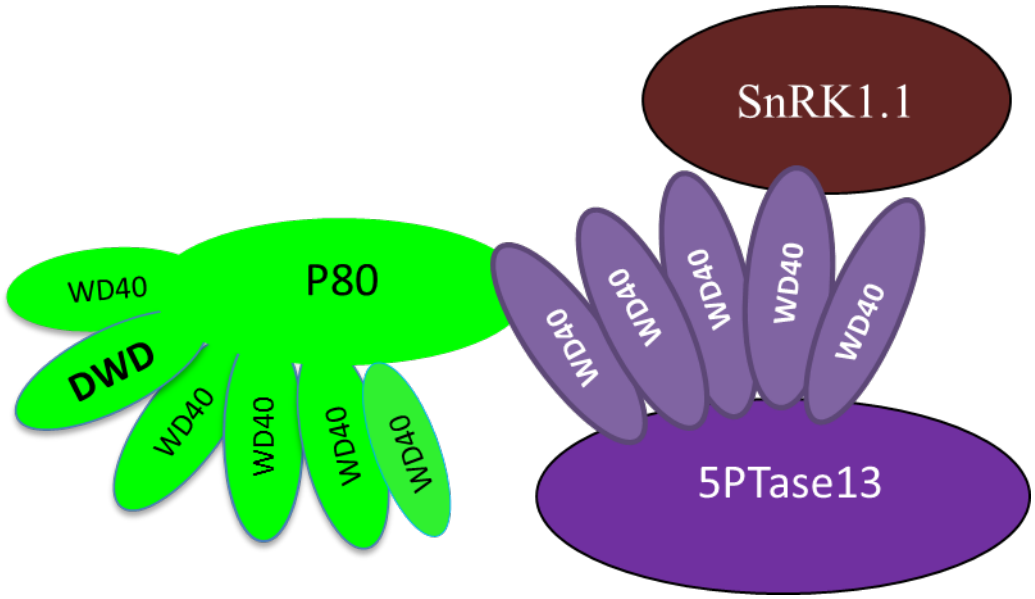

Figure 3: **Association of 5PTase13 with SnRK1.1 and P80.**

Yeast-two-hybrid screen using WD40 repeats of 5PTase13 as baits revealed two interactors, the energy sensor, SnRK1.1 and the Arabidopsis homolog of Human UAF1, called P80.

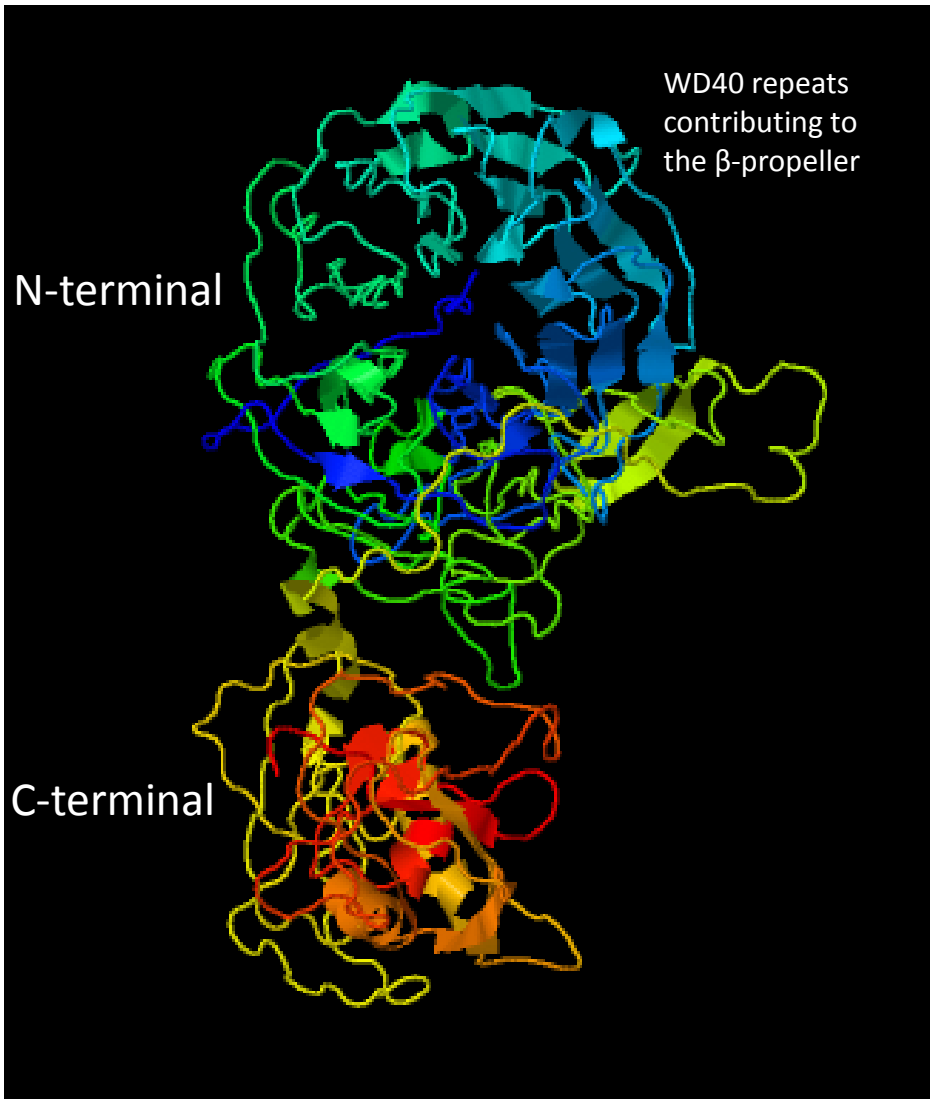

Figure 4: Phyre2 Model of Arabidopsis P80.

Figure represents the predicted structural model for Arabidopsis P80. Image is colored. Rainbow from N⟶C terminal. The WD40 repeats contribute to the propeller structure.

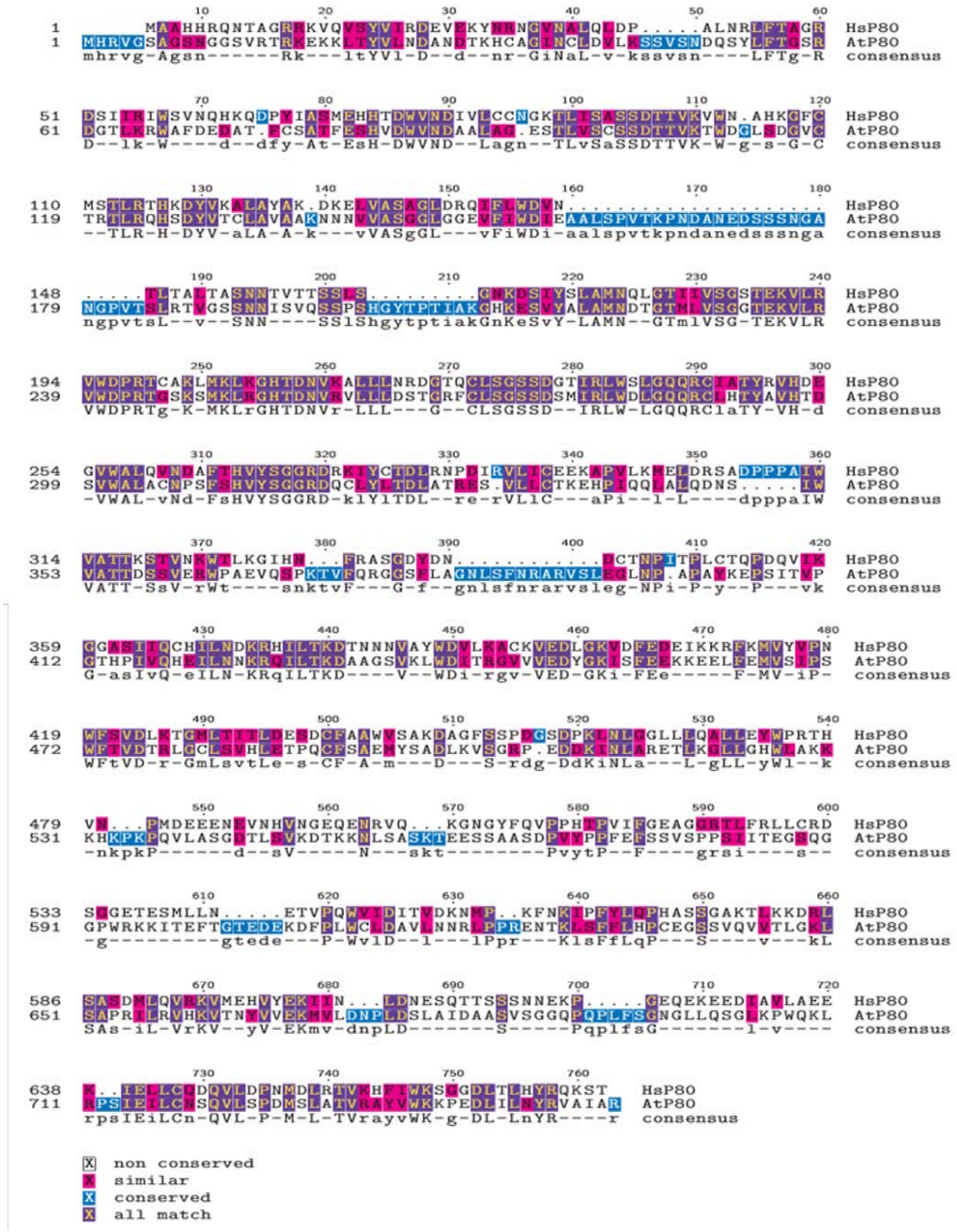

Figure 5: Alignment of Arabidopsis P80 with Human UAF1 protein.

CLUSTALW was used to align the protein sequences of Arabidopsis protein P80 with Human UAF1 protein. The proteins share 41% amino acid homology.

RATIONALE

Unpublished genetic data from the lab support the idea that the plant protein, P80 is required for SnRK1.1 function in plants. Specifically, *p80* loss-of-function mutants are similar to plants containing a knock-down of SnRK1.1 and SnRK1.2 in that they are deficient in root growth under low energy conditions and root growth is normalized by an exogenous energy source, 3% sucrose. In contrast SnRK1.1 overexpressors have better root growth in low energy conditions and become compromised when 3% sucrose is present (Baena-Gonzalez et al. 2007). The Gillaspy lab has performed an extensive analysis of mutant *p80* plants. When grown in soil *p80* mutants have an altered leaf phenotype and they senesce early (Ananieva, E., Dissertation, 2009). This is opposite in nature to SnRK1.1 overexpressors which have an extended lifespan. This reprogramming is thought to occur under low energy conditions (Baena-Gonzalez et al. 2007). In contrast, SnRK1.1 epitope-tagged with HA (hereby referred to as SnRK1.1:HA/WT) was found to have have increased vegetative biomass, most likely occurring as a result of lengthening of the vegetative phase of development (Gillaspy Lab, unpublished data). In addition, a recently published putative SnRK1.1 dominant negative mutant was shown to undergo early leaf senescence (Cho et al. 2012).

Analysis of the spatial expression patterns of the SnRK1.1 and P80 genes indicated that both genes are expressed in similar tissues. A former graduate student from the Gillaspy lab, Jenna Hess elucidated the spatial expression patterns of SnRK1.1 and SnRK1.2 using promoter:GUS constructs *in vivo*. The SnRK1.1p:GUS expression was found to be highest in the cotyledons at four days, and then in the vascular tissue and true leaves in the later stages of development. SnRK1.2p:GUS was found to have minimal expression and is restricted to developing leaf primordia, hydathodes, proximal portions of the leaves and lateral root primordia. Overall, the expression of SnRK1.1p:GUS and SnRK1.2p:GUS were determined to be limited to the same range of tissues during the course of seedling development (Hess,J., Thesis, 2011).

Other lab members were involved in the construction and analysis of P80 promoter:GUS constructs. P80 was found to be expressed in cotyledons and true leaves. It was also expressed in

the vascular tissue and lateral root primordia. Expression expanded to the root tip as well, but was not found in the root hairs.

The similarity in SnRK1.1 and P80 loss-of-function phenotypes, our promoter:GUS expression patterns and protein complex data suggest P80 and SnRK1.1 function in a related pathway. Specifically, data suggest that P80 may be required for SnRK1.1function. Thus, my thesis has focused on the question of whether P80 is required for the proper accumulation and location of SnRK1.1 in Arabidopsis.

My work has also investigated other aspects of Ins signaling in *p80* mutants. Specifically, I have examined levels of the InsPs in *p80* mutants, especially a new class of InsPs called Di- or Tri-phosphorylinositol polyphosphates (PPx-InsPs) or Ins pyrophosphates. Studies have shown that Ins pyrophosphates are altered in response to various stresses. Loss-of-function *p80* mutants display a severe stress phenotype, making it likely that the levels of PPx-InsPs in these mutants may be altered. As synthesis of Ins pyrophosphates in plants is likely catalyzed by two kinases named VIP1 and VIP2, I have also produced and characterized VIP1- and VIP2-promoter:GUS transgenic plants. This work has allowed me to provide an initial assessment of where the Arabidopsis VIP kinases are expressed, and as such, where synthesis of PPx-InsPs occurs.

STATEMENT OF OBJECTIVES

In my first objective, I examine whether P80 is required for proper accumulation and location of SnRK1. To accomplish this objective, I analyze the effects of expression of exogenous SnRK1.1:GFP and SnRK1.2:GFP transgenes under the control of 35S Cauliflower Mosaic Virus (35S CaMV) promoter in wild-type (WT) and *p80* mutant. I also address whether *p80* mutants are altered in InsPs levels. In addition, I elucidate the expression patterns of a group of genes that, we predict, function as inositol hexakisphosphate ($InsP_6$) kinases. Since these enzymes are predicted to catalyze synthesis and hydrolysis of inositol pyrophosphate bonds, they also may impact energy signaling in plants.

1. Determine the effect of overexpression of SnRK1.1 and SnRK1.2 in the *p80* mutant
2. Assess the presence of higher inositol polyphosphates in the *p80* mutant
3. Examine the expression pattern of the VIP kinases, *At*VIP1, *At*VIP2

CHAPTER II

Objective 1. To determine whether P80 is required for proper accumulation and location of SnRK1.1 and SnRK1.2

INTRODUCTION

In this study, we aim to determine the effect of the overexpression of SnRK1 proteins in the *p80* mutant as compared to its wild-type (WT) plant. In order to accomplish this aim, ectopic expression of a SnRK1.1: or SnRK1.2:GFP transgene was carried out under control of the 35S CaMV promoter in both WT and *p80* mutants. The resulting transgenic plants were screened for homozygosity. They were characterized with respect to their phenotypes, subcellular localization and expression levels of SnRK1:GFP using antibodies that recognize SnRK1 or GFP.

RESULTS

Phenotypic analysis of the effects of overexpression of SnRK1.1 and SnRK1.2 in *p80* mutants

Loss-of-function mutants of the *P80* gene display a severe growth retardation phenotype. Their rosette leaves are small and rounded. *p80* mutants are able to flower and develop siliques even though development is delayed as compared to WT plants. The overall size of *p80* mutants is smaller than WT plants. It is important to note that *p80* mutants exhibit very early senescence (Ananieva, E., Dissertation, 2009). Previous work on SnRK1.1 RNAi plants has linked both senescence and flowering time to nutrient sensing in plants (Baena-Gonzalez et al. 2007). When the SnRK1.1 RNAi plants were grown, we observed delayed development, retarded growth and smaller size. Hence, the overexpression of SnRK1 in the *p80* mutant was an approach to determine if SnRK1.1expression would alter the development of *p80* mutants. Due to close homology between SnRK1.1 and SnRK1.2, we also wanted to look at effect of overexpression of SnRK1.2 in WT and *p80* mutants.

Construction of a SnRK1.1: or SnRK1.2:GFP transgene was carried out under the control of the 35S CaMV promoter in both WT and *p80* mutants by previous members of the lab (Figure 6). For expression of SnRK1.1, a transgene directing expression of the SnRK1.1.2 splice variant was used, as this was the only known cDNA at that time. The resulting transgenic plants were screened to achieve homozygosity. All the plants were grown in a growth chamber with visible radiation between 100-130 μE and long-day conditions (16 hours light). Homozygous lines of SnRK1.1:GFP in the WT background (hereafter referred to as SnRK1.1:GFP/WT) were obtained by previous lab members. This transgenic line was analyzed for its phenotypic characteristics by Jenna Hess and Elitsa Ananieva. After genotyping and confirming the presence of the construct by sequencing, we grew the homozygous SnRK1.1:GFP/WT background and did not detect any discernible difference in growth and development as compared to the WT plants. This result was in contrast to the phenotype observed in SnRK1.1:HA/WT plants. The difference in the phenotypes of the two SnRK1.1 overexpressors may be due to the different splice variants used. Different ecotypes of WT Arabidopsis used for overexpressing SnRK1.1 could also be an explanation for this difference. A representative result of my observations is shown in Figure 7.

Figure 6: SnRK1.1 and SnRK1.2 fused to GFP constructs.

The figure shows SnRK1.1 and SnRK1.2 fused with GFP construct maps. Coding sequences of the two genes were fused to the green fluorescent protein(GFP) . This is followed by the 35S CaMV termination element (T35). Left border (LB) and Right border (RB) are indicated. The kanamycin resistance gene (BASTA^R) allows for selection of transgenic plants.

In the *p80* mutant background, we were able to obtain two independent homozygous lines of SnRK1.1:GFP (hereafter referred to as SnRK1.1/*p80*). The two lines were genotyped. We examined these two lines in their initial heterozygous states over different developmental stages. Data was collected for 15 and 21 day-old soil grown plants (data not shown). The segregating population did not exhibit any phenotypic characteristics different from the parent population. Figure 7 depicts the phenotypes observed in the two homozygous lines of SnRK1.1:GFP /*p80*.

T_0 seeds of Arabidopsis plants transformed with SnRK1.2:GFP were screened on plates with a kanamycin selection marker. Four different lines of transformants in their heterozygous stages were analyzed for phenotypic traits. 21 day-old transgenic plants grown under regular light of 100-130 μE showed more rounded leaves than WT plants (data not shown). Two independent homozygous lines were subsequently obtained and their growth and development with respect to size was analyzed. It should be noted that the homozygous lines did not show a similar rosette leaf phenotype as in the previous generation. Figure 8 shows the development of 31 day-old SnRK1.2:GFP in the WT (hereafter referred to as SnRK1.2:GFP/WT). Average rosette size of Line 3 appears to be lesser than that of Line 1. However, no obvious alteration in flowering time and silique production was observed. It should also be noted that some of the WT rosettes exhibited similar small rosettes. To gather more conclusive evidence of an alteration in phenotype, these lines have to be grown for more generations with an increased 'N' number and monitored for size.

Only one homozygous line SnRK1.2:GFP in the *p80* mutant (hereafter referred to as SnRK1.2/*p80*) was obtained. Four different heterozygous lines were grown under regular light. Analysis of the segregating population did not reveal any discernible differences in phenotypic traits when compared to its parent, the *p80* mutant. Of the four heterozygous lines, one was screened to achieve homozygosity. This transgenic line has small, rounded leaves and senesces prematurely. It has delayed flowering, small siliques and fewer seeds. Figure 9 shows 31 day-old SnRK1.2:GFP/*p80* mutant background. Some individual plants at this stage show a growth phenotype which is similar to the WT. However, further along in development, all SnRK1.2/*p80* showed a developmental phenotype similar to *p80* mutant.

Based on growth and developmental phenotypes observed, we conclude that overexpression of SnRK1.1:GFP/WT did not show any alteration in phenotypes when compared

with their parent background WT plants. The two independent lines of SnRK1.1:GFP/*p80* did not portray any traits in their growth phenotype that were different from *p80* mutants. This shows that overexpression of SnRK1.1:GFP/*p80* does not alter their growth and development. More number of plants of SnRK1.2:GFP/WT need to be grown and observed in order to conclusively state that the overexpression of this transgene affects phenotype. We conclude that SnRK1.2:GFP/*p80* does not alter the *p80* mutant phenotype. More independent lines of SnRK1.2:GFP/*p80* need to be screened to confirm this interpretation.

Figure 7: Phenotype of SnRK1.1:GFP in Wild-type background.

Figure shows a representative photograph of phenotypes observed in 31 day-old SnRK1.1:GFP/WT (N=18). No discernible differences in phenotype between the WT and the transgenic line were observed during development.

Figure 8: Phenotype of SnRK1.1:GFP in *p80* mutant background.

Figure shows a representative photograph of phenotypes observed in 31day-old SnRK1.1:GFP/ *p80* (N=18). No discernible differences in phenotype between the *p80* mutant and the transgenic lines expressing SnRK1.1:GFP/*p80* were observed during development.

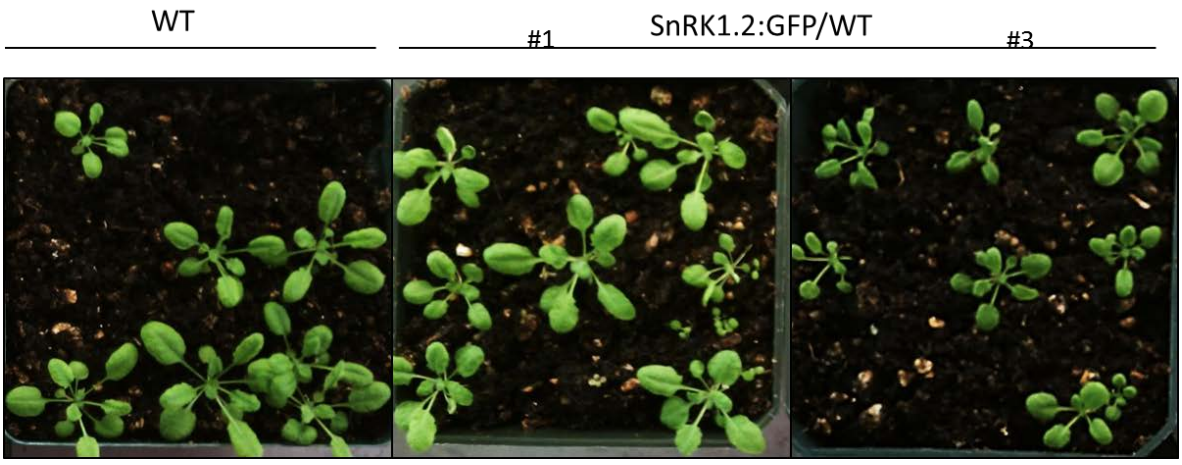

Figure 9: Phenotype of SnRK1.2:GFP in Wild-type background.

Figure shows a representative photograph of phenotype observed in 31 day-old SnRK1.2:GFP/WT (N=18). No discernible differences were observed in line #1 as compared to the wild-type. Phenotype of line #3 appears to be smaller than that of the WT. More plants with a higher 'N' number need to be analyzed in order to state conclusively if the overexpression of SnRK1.2:GFP is playing a role in the altering of the phenotype of the plant.

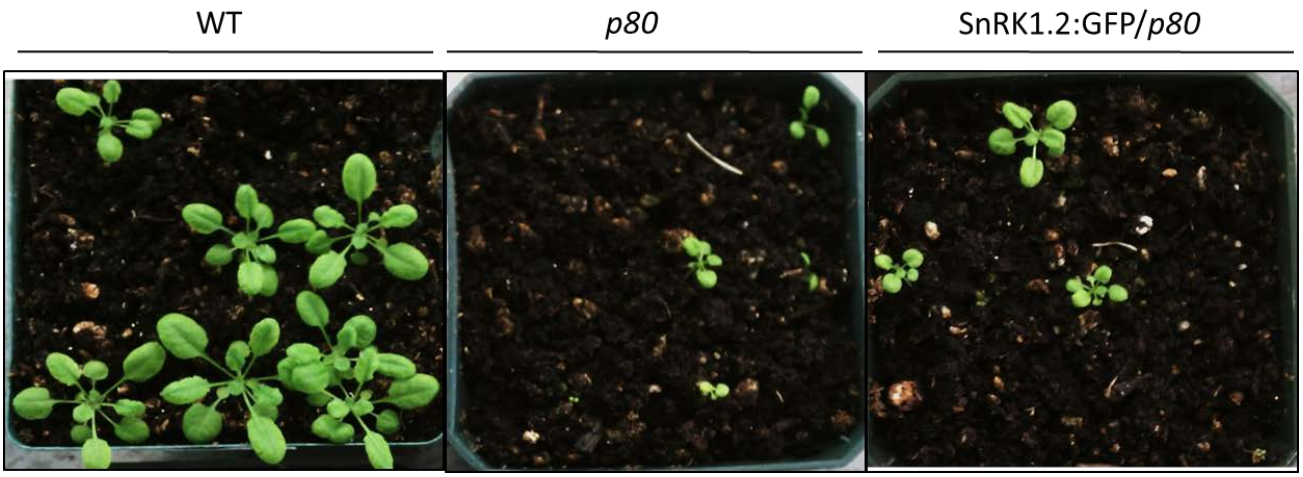

Figure 10: Phenotype of SnRK1.2:GFP in *p80* mutant background.

Figure shows a representative photograph of phenotype observed in 31 day-old SnRK1.2:GFP/*p80* (N=18). No discernible differences in phenotype between *p80* mutant and the transgenic line expressing SnRK1.2:GFP/*p80* were observed during development.

Subcellular localization of SnRK1.1:GFP and SnRK1.2:GFP in *p80* mutants

In order to understand if P80 plays a role in the proper subcellular localization of SnRK1, the expression of SnRK1:GFP was examined in WT, as well as in *p80* mutants. If P80 is required for proper localization of SnRK1, then a difference can be expected to be seen in the subcellular localization of SnRK1:GFP/*p80* mutant seedlings *in vivo.* This experiment was conducted in collaboration with another Gillaspy lab member, Phoebe Williams.

The seedlings were grown on agar plates supplemented with 0.5x MS + 1% sucrose. Using a Zeiss microscope that is equipped with fluorescence optics, we were able to detect SnRK1:GFP fluorescence in both WT and *p80* mutant seedlings. We examined two developmental stages of the seedlings, very early at four days and a later stage, eleven days. We also examined tissues, mainly rosette leaves of 25 day-old soil-grown mature plants. We did this to test whether P80 alters the subcellular localization of SnRK1 during development. This was done to see if there is any alteration of SnRK1 localization at later stages when the plants are developing inflorescences. This experiment was done once using different homozygous lines of the transgenic plants, hence the data presented should be treated as preliminary. Strong fluorescence of SnRK1.1 tagged with GFP was detected in the nuclei and cytoplasm of guard cells within four day-old WT seedlings (Figure 11A). Neither of the two transgenic lines expressing SnRK1.1 tagged with GFP in the *p80* mutant background showed SnRK1.1:GFP fluorescence in the cytoplasm or the nuclei of the guard cells (Figure 11C). Analysis performed on eleven day-old seedlings showed strong expression in the guard cells of seedlings with SnRK1.1:GFP/WT background (Figure 11E) but no detectable GFP in the same aged SnRK1.1:GFP/*p80* seedlings (Figure 11G). Also, from eleven day-old seedlings, we were able to detect GFP signal in cytoplasm and chloroplasts of cells within the hypocotyl of both SnRK1.1:GFP/*p80* and SnRK1.1/WT (data not shown). When 25 day-old mature soil-grown plants were examined, the GFP signal was observed only in the cytoplasm and not in the nuclei within SnRK1.1:GFP/WT (Figure 11I). No GFP signal was observed in the guard cells of 25 day-old mature soil-grown pants of SnRK1.1:GFP/*p80*.

We conclude from preliminary data that SnRK1.1:GFP is expressed in the cytoplasm and nuclei within guard cells in WT seedlings. In comparison, it is harder to detect SnRK1.1:GFP

fluorescence in SnRK1.1:GFP/*p80* appears to have less GFP fluorescence in the guard cells. This suggests that presence of P80 impacts the level of SnRK1.1:GFP. The lack of nuclear signal in mature tissues of SnRK1.1/WT suggests that SnRK1.1 may not be expressed in the same location in every cell throughout the life cycle of the plant. This experimental approach would be strengthened by repeating and confirming the subcellular localization needs to be done using specific organelle markers.

To test how P80 impacts SnRK1.2, we examined SnRK1.2 tagged with GFP overexpressed in *p80* mutants and WT plants. Two different stages of seedlings, at 4 days and at eleven days were examined. These seedlings were grown on 0.5x MS agar + 1% sucrose. 25-days old mature leaf tissues grown on soil were also examined. We were able to detect faint signal in the nuclei of the root tips of 4 days-old seedlings (Figure 12A). In comparison, we were able to detect abundant signal in the root tip nuclei (Figure 12C). Examination of 11 day-old seedlings expressing SnRK1.2 tagged with GFP in WT seedlings showed very faint root nuclei signal (Figure 12E). In comparison, SnRK1.2:GFP/*p80* mutants fluorescence signal in 11 day-old seedlings was very intense (Figure 12G). We could not detect expression of SnRK1.2:GFP in either WT or *p80* mutant backgrounds in leaf tissue from mature 25-day-old soil grown plants.

We conclude that SnRK1.2:GFP was expressed in the root nuclei of both *p80* and WT seedlings. Even though the level of SnRK1.2:GFP/*p80* was greater as compared to WT, the subcellular localization did not vary. We conclude that the major role of P80 is to impact the abundance of SnRK1.2.

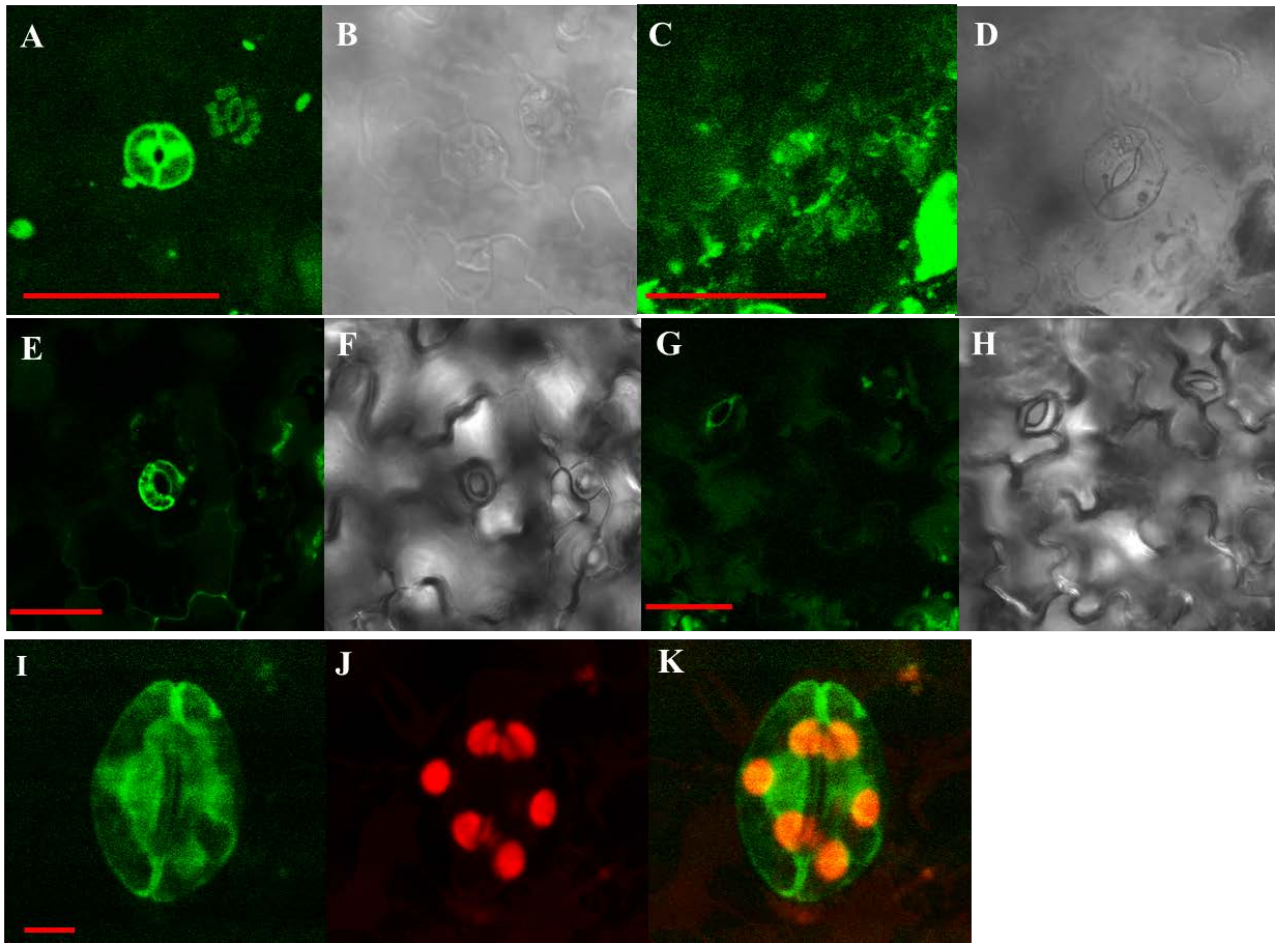

Figure 11: Subcellular localization of SnRK1.1:GFP.

Confocal imaging of SnRK1.1:GFP fluorescence in 4 day-old (A) WT, (C) *p80* mutant seedlings and 11 day-old (E) WT and (G) *p80* mutant seedlings. Panels (B), (D), (F) and (H) show the corresponding differential interference contrast images. Panel (I) shows autofluorescence of chlorophyll of 4-week old SnRK1.1:GFP in wild-type background plants grown in soil. Panel (J) shows the fluorescence emitted above 560 nm. (K) shows the merged image of (I) and (J). Excitation for GFP was done at 488nm using an Argon laser and emission was measured between 505 nm to 550 nm. Scale bars = 50 μm (A-H), 5 μm (I-J)

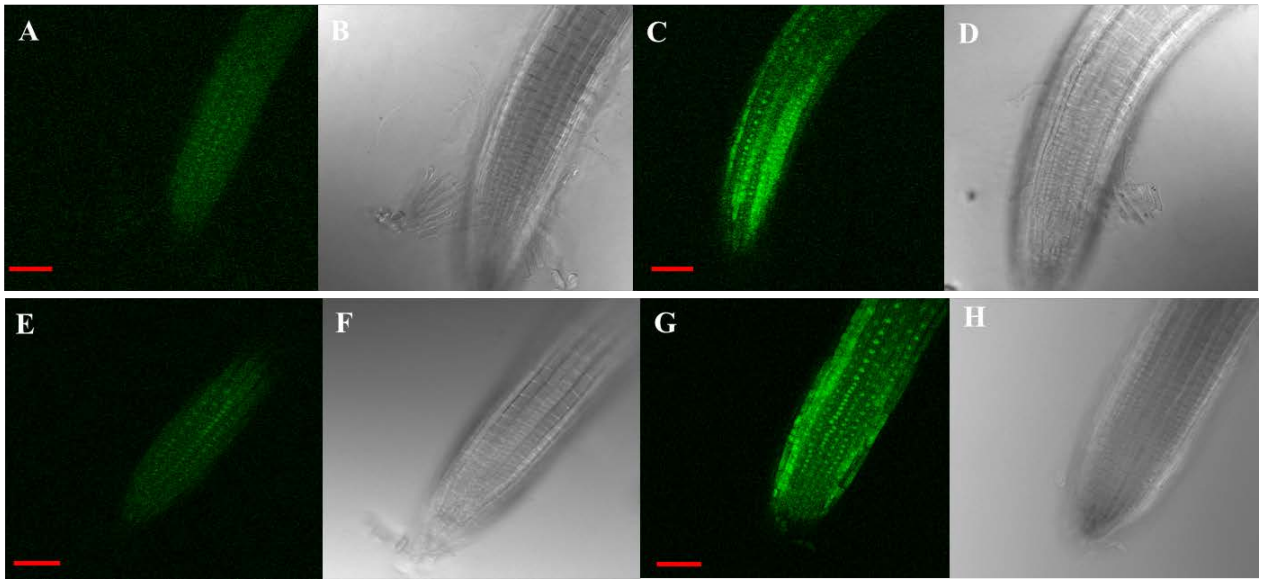

Figure 12: Subcellular localization of SnRK1.2:GFP.

Confocal imaging of SnRK1.2:GFP fluorescence in 4 day-old (A) WT, (C) *p80* mutant seedlings and 11 day-old (E) WT and (G) *p80* mutant seedlings. (B), (D), (F) and (H) present the corresponding differential interference contrast images. Excitation for GFP was done at 488 nm using an Argon laser and emission was measured between 505 nm to 550 nm. Scale bar = 50 µm

Detection of SnRK1 protein in wild-type and *p80* mutants

The human P80 homolog, UAF1 is part of a protein complex that is involved in the deubiquitination of proteins, thus playing a role in their regulation. We hypothesize that P80 in Arabidopsis plays a similar role making it important to address if SnRK1.1 is regulated via a P80 deubiquitination complex. The predictive model from this hypothesis states that P80, as part of a deubiquitination complex, aids in the removal of ubiquitin molecules from SnRK1.1, resulting in its protection from the 26S proteasome.

This hypothesis implies that mutants in P80 will have an alteration in the stability of SnRK1. Genetic data from our lab suggest that *p80* mutants may have an alteration in their SnRK1 protein levels. A previous student from our lab, Jenna Hess, generated an antibody against SnRK1.1. She also tested the effectiveness of the antibody against native SnRK1.1. She was able to determine that the antibody was specific to SnRK1.1 and detects both native SnRK1.1 and transgenic SnRK1.1 fused to GFP. In order to test the hypothesis that *p80* mutants will have an alteration in their SnRK1 levels, anti-SnRK1.1 and anti-GFP antibodies were used to detect protein levels in WT tissue, *p80* mutants and in SnRK1 transgenic lines. A change in the SnRK1 levels between the WT and the *p80* mutant will be a step further to suggest that SnRK1 levels are regulated by P80 through a post-translational mechanism.

Western blot analyses were performed on 11 day-old seedlings that were grown on 0.5x MS + 1% sucrose. The samples were extracted with homogenization buffer containing a protease inhibitor and probed using an anti-GFP antibody (Rockland Immunochemicals Inc.). This was done in order to confirm the presence of intact transgenic SnRK1:GFP protein in the overexpressing lines. Bradford assay was performed to ensure equal loading of the protein samples (Bradford 1976). Each well was loaded with 30 μg of protein.

When probed with an anti-GFP antibody, signal was detected in the lane loaded with extract from SnRK1.1:GFP/WT, at the expected size, about 86 kDa molecular mass. SnRK1.2:GFP/*p80* mutant background was also detected at its expected size of about 83 kDa (Figure 13A). No transgenic protein using the anti-GFP antibody was detected in other samples, namely SnRK1.1:GFP/*p80* mutant background and SnRK1.2:GFP/WT background.

All the samples were also probed using the anti-SnRK1.1 antibody to detect native SnRK1.1 protein. Native SnRK1 protein was detected in all the sample lanes (Figure 13B). Transgenic SnRK1.1:GFP was detected in the WT background but not in the *p80* mutants background using the anti-SnRK1.1 antibody. The amount of native SnRK1 protein detected in wild-type15 (WT15) lane is less than the other wild-type, CS908. This could be due to some inequality in loading of protein samples in each of the lanes. Lower expression of native SnRK1 was detected in SnRK1.2:GFP/WT (1). This might be due to lower expression of native SnRK1.

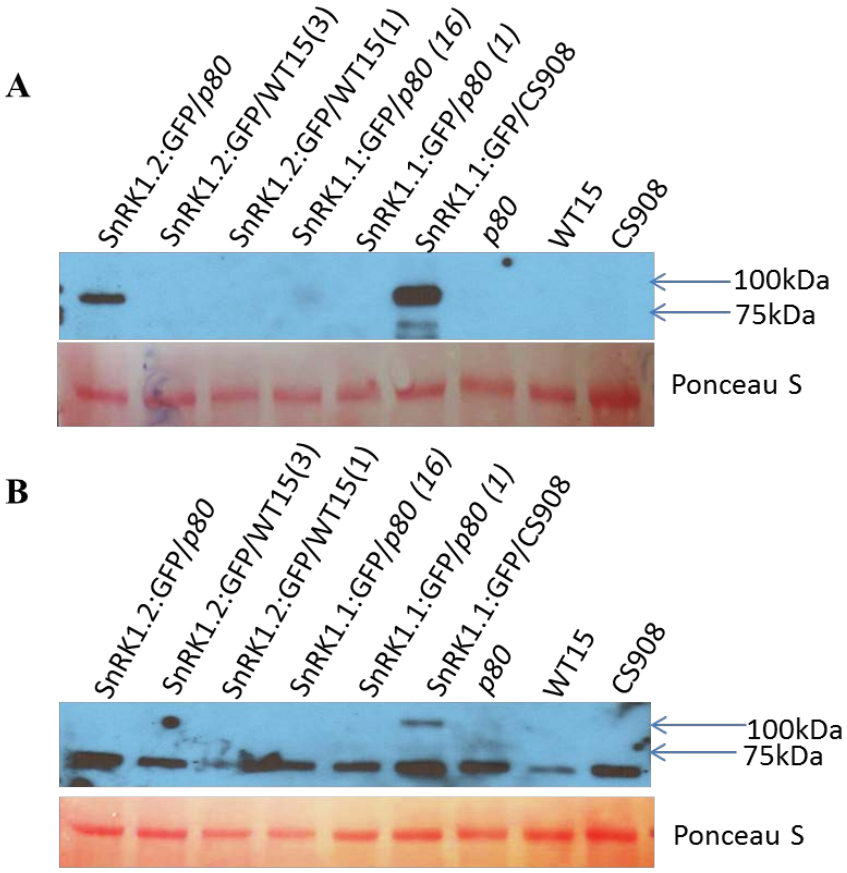

Figure 13: Western Blot Analysis of transgenic and native SnRK1 protein levels.

A Western Blot was performed to detect (A) transgenic SnRK1:GFP protein using Anti-GFP antibody and (B) native SnRK1.1 protein using Anti-SnRK1.1 antibody

RNA analysis of SnRK1.1 and SnRK1.2 transgene in wild-type and *p80* mutants

A previous Gillaspy lab analysis of SnRK1.1 RNA expression indicated no significant difference in SnRK1.1 levels between WT and *p80* mutants (data not shown). However, in this analysis, PCR primers used are expected to amplify all three isoforms of SnRK1.1.

As seen in Figure 13, there was no accumulation of SnRK1.2:GFP in SnRK1.2:GFP/WT plants and similarly, there was no accumulation of SnRK1.1:GFP protein in SnRK1.1:GFP/*p80* plants. Therefore, we tested whether these transgenic plants were accumulating SnRK1.1:GFP or SnRK1.2:GFP RNA. If the RNA levels are similar in all the samples, then this will be an indication that the presence or absence of P80 affects the accumulation of transgenic protein levels of SnRK1. Quantitative real-time polymerase chain reaction (qRT-PCR) was performed to detect the SnRK1.1:GFP or SnRK1.2:GFP transcript levels. Total RNA was extracted from 11 day-old seedlings, grown on 0.5x MS + 1% sucrose and cDNA synthesized using reverse transcriptase. Amplification of the GFP coding region present in the transgene was achieved using specific forward and reverse primers and annealing temperatures. Peroxisomal Ubiquitin 4 (PEX4) gene was used as an endogenous control to normalize the data. Each reaction was performed in triplicates and the error was calculated as standard deviation of the mean of the three reactions.

SnRK1.1:GFP RNA was detected in SnRK1.1:GFP/WT plant tissue and used to compare the other transcripts. While SnRK1.1:GFP RNA was abundant in SnRK1.1:GFP/WT, the transcript of SnRK1.1:GFP in SnRK1.1/*p80* mutant background is about four-fold lower. Low levels of transcript were detected in both of the two lines of SnRK1.2:GFP/WT while the RNA levels of SnRK1.2/*p80* mutant background are elevated. The conclusion drawn from this experiment is that P80 also impacts the relative amount of SnRK1.1:GFP and SnRK1.2:GFP. Together, the data in Figures 13 and 14 indicate that the changes in the level of accumulation of SnRK1.1 and SnRK1.2:GFP protein correlate with the amount of RNA detected in each of the samples.

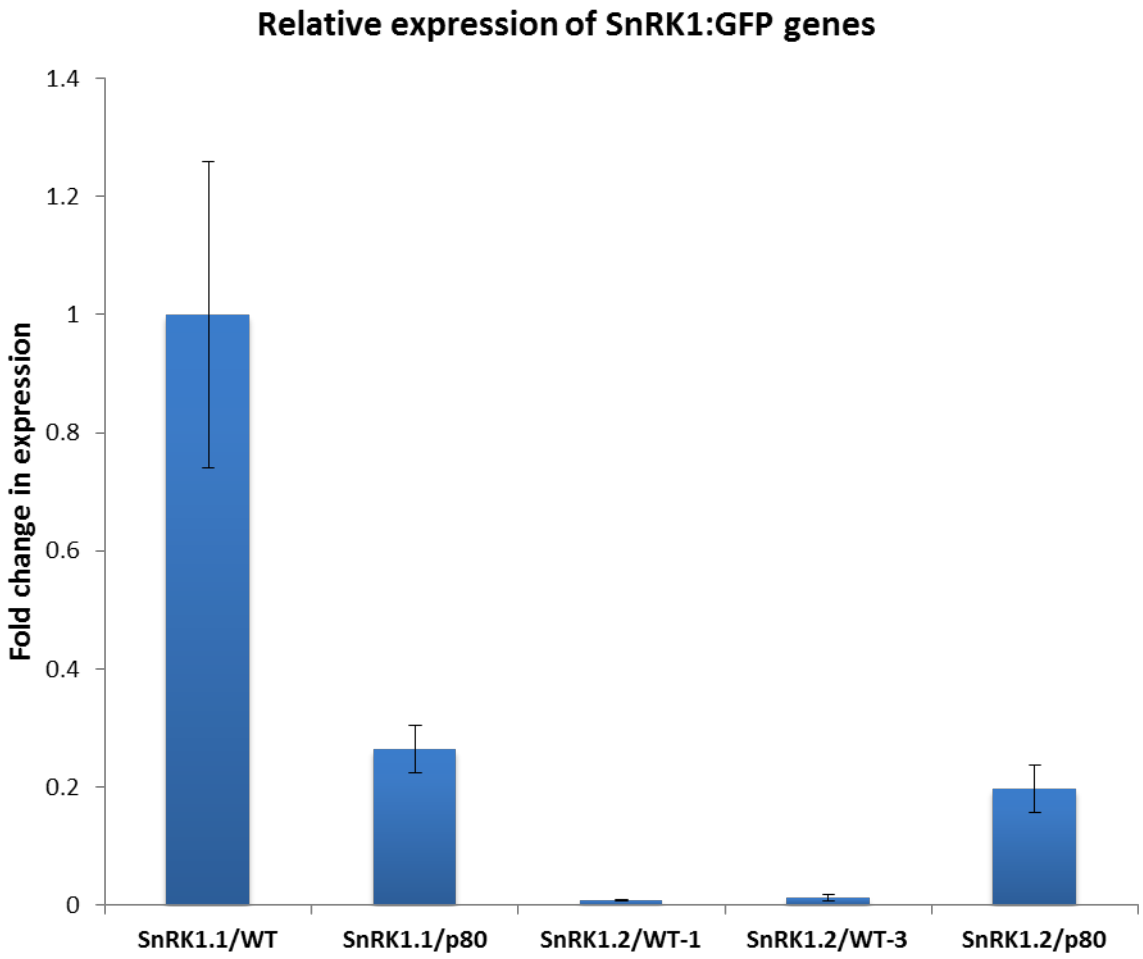

Figure 14: Relative Expression of SnRK1:GFP genes.

Quantitative Real Time PCR was performed to detect transcript levels of the transgenes in WT and *p80* mutants using GFP forward and reverse primers. Real time PCR amplification curves were compared with standard curves *PEX4* gene amplification to determine expression levels. Error bars represent ± standard deviation of the mean.

DISCUSSION

Recent data have indicated the interconnection of energy and nutrient signals with Ins metabolism and signaling. The study characterizing the function of the WD repeats of 5PTase 13 in Arabidopsis revealed two binding partners: the energy sensor SnRK1.1 and the protein P80. While a physical interaction between SnRK1.1 and P80 has not been confirmed, it is interesting to hypothesize that together they play an important role in the Ins signaling pathway. Data from the Gillaspy lab indicates that P80 is part of a deubiquitinating enzyme complex. Studies from the lab have also shown that P80 may be involved in nutrient sensing and response. Data from the Gillaspy lab and review of literature shows that the SnRK1 protein affects nutrient sensing and stress signaling in plants (Baena-Gonzalez et al. 2007). This leads to the hypothesis that P80 may play a role in impacting SnRK1.1.

In order to address this hypothesis, the effects of overexpression of SnRK1.1:GFP or SnRK1.2:GFP in the *p80* mutant was analyzed. Phenotypic analyses indicated that the overexpression of either transgene, SnRK1.1:GFP or SnRK1.2:GFP in the *p80* mutant background does not affect the distinct phenotype exhibited by the *p80* mutant. These transgenic lines exhibited small, rounded leaves, early senescence and set very few seeds. The overexpression of the transgenes in the WT did not alter the normal growth and development either. One line expressing SnRK1.2:GFP in the wild-type background showed smaller rosette diameter as compared to the second line. This could be due to variability in growth conditions, like light and humidity differences. More plants of this line need to be grown in significantly high numbers and compared for size and development in order to conclusively state that the overexpression of SnRK1.2:GFP may be impacting the growth and development.

Preliminary analysis of subcellular localization of SnRK1.1:GFP revealed that SnRK1.1:GFP is expressed in the wild-type more abundantly than in the *p80* mutant. SnRK1.1:GFP expression was very high in nuclei and cytoplasm of guard cells in the WT background. Expression was also seen in chloroplasts and the cytoplasm of the hypocotyl. In comparison, SnRK1.1:GFP expression was not abundant in the guard cells in the *p80* mutant background. SnRK1.1 abundance changes with different genetic background suggesting that the accumulation of SnRK1.1 is impacted by P80. My analyses showed that the difference in

abundance could be due to reduced transcript and protein levels as noted in Figure 13 and Figure 14. Comparison of SnRK1.1:GFP and SnRK1.2:GFP transcript and protein accumulation levels reveals that SnRK1.1:GFP protein turnover may also be regulated by P80. Support for this data also comes from the fact that SnRK1.1:GFP protein levels are lower than expected levels, given the abundance of the SnRK1.1:GFP transcript levels. These experiments have to be repeated along with markers for subcellular localization.

It is interesting to note that SnRK1.2:GFP was expressed in the in the nuclei of root cells of SnRK1.2:GFP/*p80*. I did not detect any expression in the guard cell nuclei in these mutants. We were able to detect faint expression of GFP in the nuclei of roots of SnRK1.2:GFP/WT. This indicates that P80 is important for the abundance of SnRK1.2:GFP protein. These data also indicate that the SnRK1.1 and SnRK1.2 splice variants used in this work accumulated in different cell types.

We used western blotting to detect transgenic SnRK1:GFP protein in all the tissues using anti-GFP antibody. We were able to detect SnRK1.1:GFP in SnRK1.1:GFP/WT and SnRK1.2:GFP in SnRK1.2:GFP/*p80* plants. No protein was detected in any of the other lines. Probing with anti-SnRK1.1 antibody showed the presence of native SnRK1 in all the samples. The native antibody cross-reacted with SnRK1.1:GFP in SnRK1.1:GFP/WT plants. The expression of native SnRK1 in all the samples analyzed suggests that the regulation of transgenic protein might be different from that of native SnRK1.

A final speculation that could be made is that the splice variant used for the construction of SnRK1 transgenes might be very important. Specifically, SnRK1.1.2, may not the most abundant isoform found in the cell. The splice variant, SnRK1.1.3 is likely to be the most abundant isoform and does not contain a stretch of 23 AA in its N-terminal that is present in the splice variant used in my work. One implication of my work is that SnRK1.1.2 variant is regulated different than the native SnRK1 protein accumulated in the cell as seen by western blotting. Further, work discussed here and other unpublished data show the native SnRK1 protein is not affected by the presence and absence of P80. Comparison of the various SnRK1 splice variant will help delineate the way in which P80 may impact SnRK1 protein.

CHAPTER III

Objective 2: Assess the presence of higher Inositol polyphosphates in the *p80* mutant

INTRODUCTION

There is recent evidence that another group of InsPs may also have a role in signaling. These are a novel group of Inositol pyrophosphates containing diphospho or tri-phospho moieties (PPx) on the inositol ring (Shears et al. 2011). Characterization of diphosphoinositol pentakisphosphate ($InsP_7$) and bisdiphosphoinositol tetrakisphosphate ($InsP_8$) signaling was first elucidated in *Dictyostelium* chemotaxis in response to a cAMP produced in neighboring cells (Luo et al. 2003). These higher inositol pyrophosphates have been implicated in several biological processes in animals and humans such as transcriptional regulation, chromatin remodeling, telomere maintenance and homeostasis (Tsui et al. 2010; Boss et al. 2012). Recently, it has been found that PPx-InsPs influence the transcription of glycolytic genes and function of mitochondria, thus controlling metabolism (Szijgyarto et al. 2011). $InsP_7$ levels have also been found to increase during phosphate starvation in yeast, ultimately leading to expression of those genes that are required to maintain cellular homeostasis (Lee et al. 2007). In animals, PPx-InsPs have been shown to be involved in embryonic development, fertility and insulin signaling (Tsui et al. 2010).

PPx-InsPs contain a linear chain of two (PP) or three (PPP) phosphates and may be involved in serving a function analogous to ATP, in communication of nutrient status, as they do in yeast (Kane et al. 2000; Boer et al. 2010). In fact, $InsP_7$ serves as a phosphate donor for covalent modifications of proteins (Saiardi et al. 2004).

Even though plant seeds contain the most abundant source of $InsP_6$, the precursors of PPx-InsPs, these PPx-InsPs have not been fully characterized in plants to date. Two reports in the literature illustrate the presence of molecules eluting from HPLC gradients that are more polar than $InsP_6$ (Flores et al. 2000; Dorsch et al. 2003). My second objective focuses on assesing the presence of these unique Ins phosphate signaling molecules, $InsP_7$ and $InsP_8$ in plants. My goal was to follow up on these initial reports and quantify these PPx-InsPs from plant tissues.

PPx-InsPs have been known to be altered in response to stress (Lee et al. 2007). Mutants in P80 exhibit a severely stressed phenotype. Hence, we hypothesize that *p80* mutants may be altered in PPx-InsPs levels.

The work described in this section addresses the following questions:

- Do vegetative tissues from plants synthesize $InsP_7$ and $InsP_8$?
- Do seeds from plants make $InsP_7$ and $InsP_8$?
- Is the Arabidopsis *p80* mutant altered in higher InsP accumulation?
- Are mutants in the $InsP_7$ synthesis enzymes altered in $InsP_7$?

RESULTS

Inositol Profiling of WT Arabidopsis

The profiling of different InsPs was done using anion exchange High Pressure Liquid Chromatography (HPLC) as described in Materials and Methods.

Eukaryotic cells have the ability to incorporate ^{3}H-*myo*-inositol from extracellular media. It is incorporated into InsPs via different phosphorylation and dephosphorylation reactions. To introduce the ^{3}H-*myo*-inositol plant tissues were incubated with ^{3}H-*myo*-inositol for 4 days in the presence of light and then extracted the InsPs according to the protocol from Azevedo et al (2006). The extracted samples containing the radiolabelled InsPs were resolved using strong anion exchange HPLC.

To carry out the Ins profiling of WT CS60000 seedlings, 4 day-old seedlings were chosen and radiolabelled with ^{3}H-*myo*-inositol for four days at room temperature. After washing off the excess radiolabel, acidic extraction was carried out followed by neutralization. Samples were loaded onto the column and eluted using an ammonium phosphate gradient as described in Materials and Methods. Radioactivity is detected using an IN/US systems radiation detector.

Figure 15 shows the HPLC trace analysis of WT seedlings. The trace in blue color shows the elution times of known standards, Ins (1) P, Ins(1,4,5)P_3 and Ins(1,3,4,5)P_4. Standards for $InsP_6$ and $InsP_7$ are being synthesized in the Gillaspy lab. The eluted fractions are collected and analyzed using a scintillation counter to increase the sensitivity of detection and to quantify the eluted InsPs. Inset of Figure 15 shows the scintillation count trace of the eluted fractions, mainly $InsP_5$, $InsP_6$ and $InsP_7$. Wild-type seedlings showed an elution profile including different InsPs. Six independent runs were used to calculate the amount of InsPs present in the vegetative tissue of Arabidopsis. The normalization of the amount of InsPs is described in Materials and Methods. $InsP_5$ and $InsP_6$ constitute 2.9% and 23.3% respectively, of all InsPs detected. $InsP_7$, a novel compound in higher plants, constitutes about 0.8% of all InsPs detected. Seedlings also showed a high amount of lower InsPs. These lower InsPs have not been quantified.

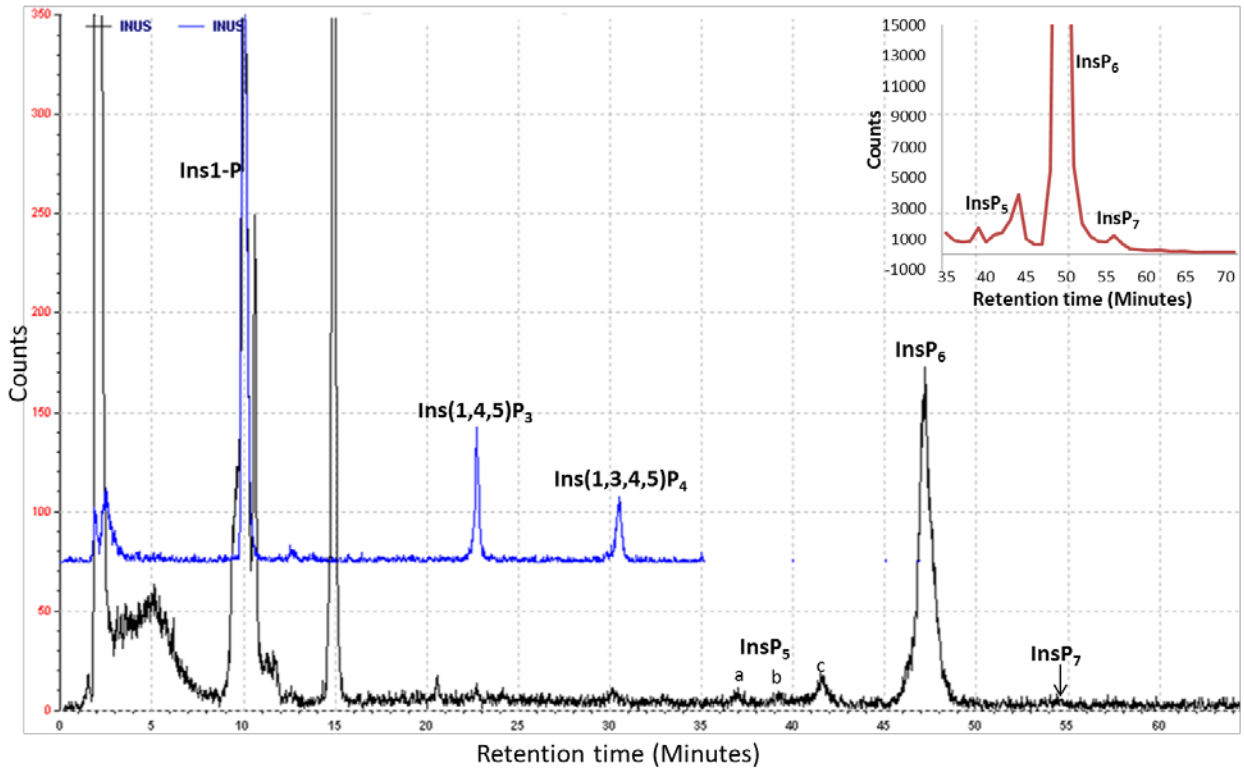

Figure 15: HPLC trace analysis of InsPs of 4 day-old WT Columbia seedlings.

The seedlings were radiolabelled with ^{3}H-*myo*-inositol, extracted and separated using a Partisphere SAX anion exchange column. Three distinct peaks for $InsP_5$, namely a,b and c and one for $InsP_6$ were identified. A discrete peak for $InsP_7$ was also identified, novel for higher plants. The blue colored trace shows the elution times for known standards. **Inset:** Figure presents the scintillation counts of the trace. Fractions eluted from the HPLC are collected and analyzed independently using a scintillation counter.

For labeling of siliques, 6-8 green siliques were chosen and radiolabeled ^{3}H-*myo*-inositol for 4 days. Figure 16 shows the elution profile of WT Arabidopsis siliques with $InsP_6$ constituting about 75% of all InsPs. $InsP_5$, its precursor constituted about 4.16%. $InsP_7$ was detected after $InsP_6$ was eluted. This PPx-InsP comprised of about 2.6% of all inositol polyphosphates detected.

We conclude that developing seeds show an increased concentration of $InsP_6$ when compared to seedlings. $InsP_7$ detected in developing seeds was also more than two times greater than in seedlings. No $InsP_8$ was detected in either seedlings or developing seeds. Figure 17 is the graphical representation of the amount of $InsP_5$, $InsP_6$ and $InsP_7$ found in seedlings and developing seeds.

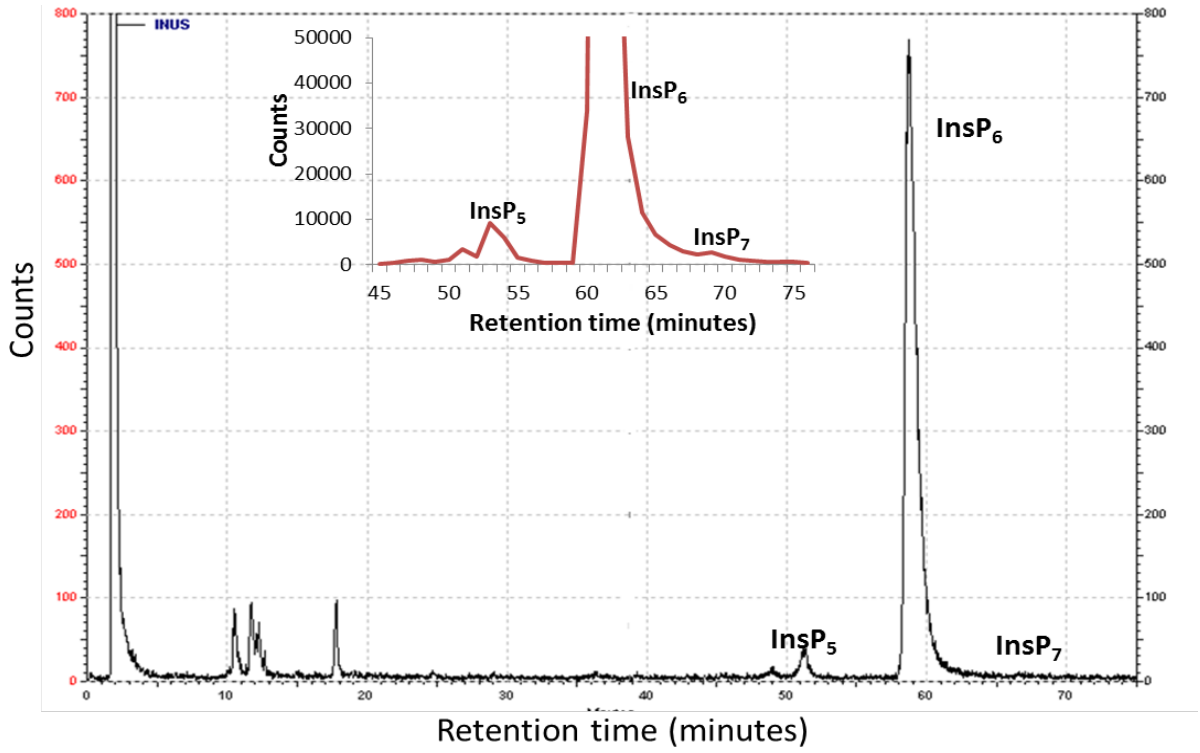

Figure 16: HPLC trace analysis of InsPs of WT Columbia developing seeds.

Wild-type siliques were radiolabelled with ^{3}H-*myo*-inositol, extracted and separated using the Partisphere SAX anion exchange column. Distinct peaks for $InsP_5$ and $InsP_6$ were identified. A discrete peak for $InsP_7$ was also identified, novel for higher plants. **Inset:** Figure presents the scintillation counts of the trace. Fractions eluted from the HPLC are collected and analyzed independently using a scintillation counter.

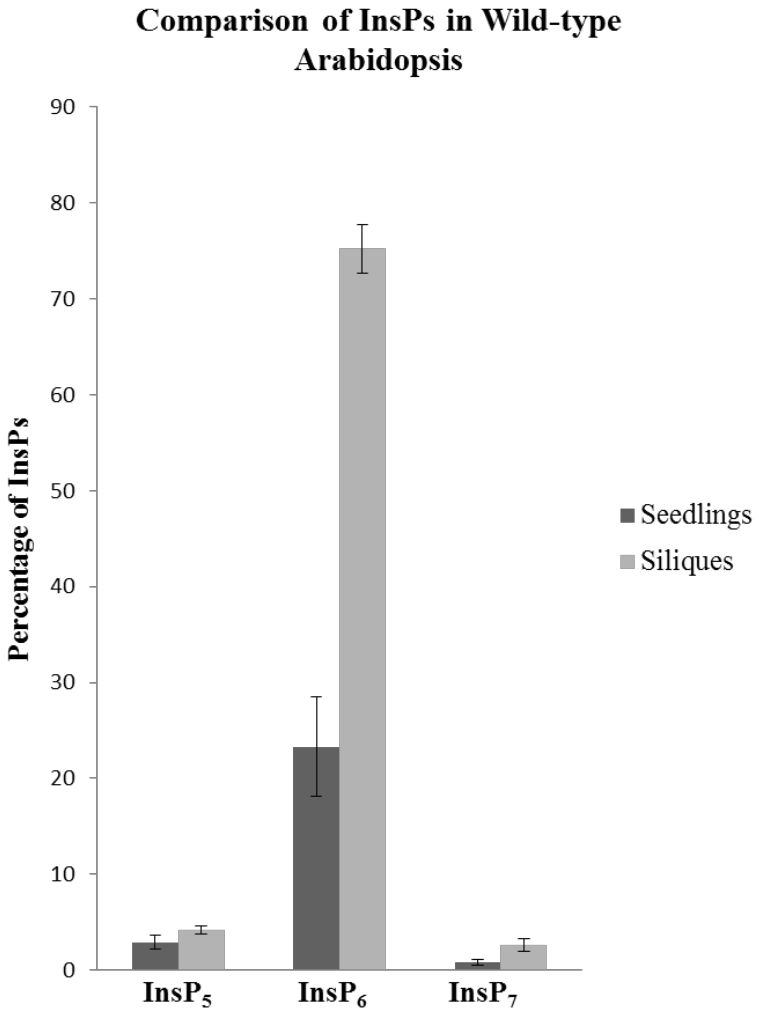

Figure 17: Graphical presentation of the percentage of amount of InsPs found in WT Arabidopsis.

Wild-type samples were radiolabelled with 100 µCi of ^{3}H-*myo*-inositol for 4 days, extracted and separated using Partisphere SAX anion exchange column. The amount of radiolabelled InsPs seedlings was compared to the amount in siliques. The error bars indicate standard deviation of the mean.

Inositol Profiling of *p80* mutant

The inositol profiling of the *p80* mutant siliques and seedlings was done as described previously. The *p80* mutant siliques (Figure 18) showed an alteration in PPx-InsPs. When compared to their wild-types, developing seeds of *p80* mutant showed an increase of about 2.4 times the amount of $InsP_7$. There was a significant decrease in the levels of $InsP_6$. $InsP_6$ is known to be involved in energy storage, seed germination and viability (Raboy 1997). Interestingly, the level of $InsP_5$ in WT was significantly lower than *p80* mutant. Inset of the figure shows the scintillation count trace of the fractions eluting $InsP_5$, $InsP_6$ and $InsP_7$. Preliminary analysis of *p80* mutants complemented with P80:GFP indicated WT amounts of $InsP_6$ and $InsP_7$ (Figure 19).

Inositol profiling of *p80* mutant seedlings shows $InsP_7$ level is about two times higher than that of wild-type seedlings. Other InsPs, $InsP_6$ are also elevated in the *p80* mutant seedlings as compared to its WT counterpart. However, this difference was not statistically significant. There is an elevation of $InsP_5$ also observed. Figure 20 depicts the HPLC trace of *p80* mutant seedlings. It shows the presence of other lower InsPs at the elution times of $InsP_4$, $InsP_3$, $InsP_2$ and InsP. Inset of the figure shows the scintillation count trace of the fractions of $InsP_5$, $InsP_6$ and $InsP_7$. Figure 21 graphically compares the amount of InsPs found in both seedlings and developing seeds of *p80* mutants with WT. Preliminary analysis of *p80* mutant seedlings complemented with P80:GFP indicated WT levels of $InsP_6$ and $InsP_7$ (data not shown).

In conclusion, we were able to observe significant differences in amounts of InsPs between WT and *p80* mutant developing seeds ($P \leq 0.05$). We were not able to observe similar significant differences in $InsP_5$ and $InsP_6$ in seedlings between the two genotypes. However, the amount of $InsP_7$ was significantly higher in *p80* mutant seedlings as compared to WT ($P \leq 0.01$).

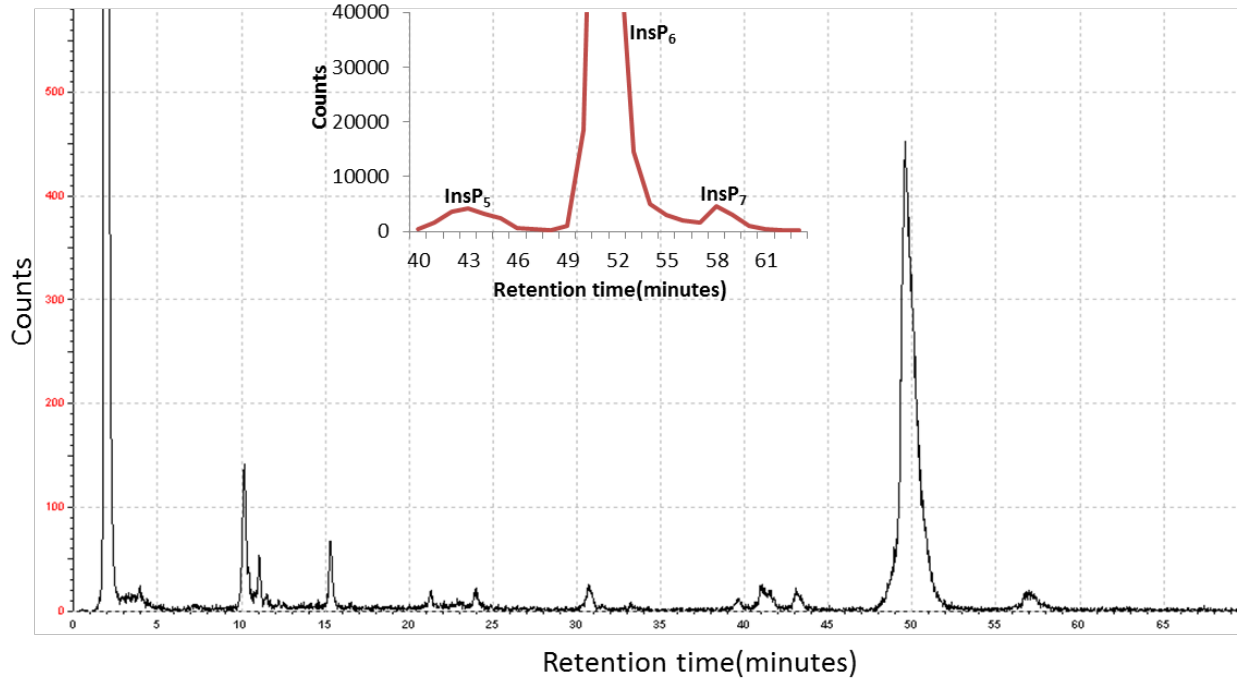

Figure 18: HPLC trace analysis of InsPs of *p80* mutant developing seeds.

Mutant *p80* siliques were radiolabelled with ^{3}H-*myo*-inositol, extracted and separated using a Partisphere SAX anion exchange column. Distinct peaks for $InsP_5$ and $InsP_6$ were identified. A discrete peak for $InsP_7$ was also identified, novel for higher plants. **Inset:** Figure presents the scintillation counts of the trace. Fractions eluted from the HPLC are collected and analyzed independently using a scintillation counter.

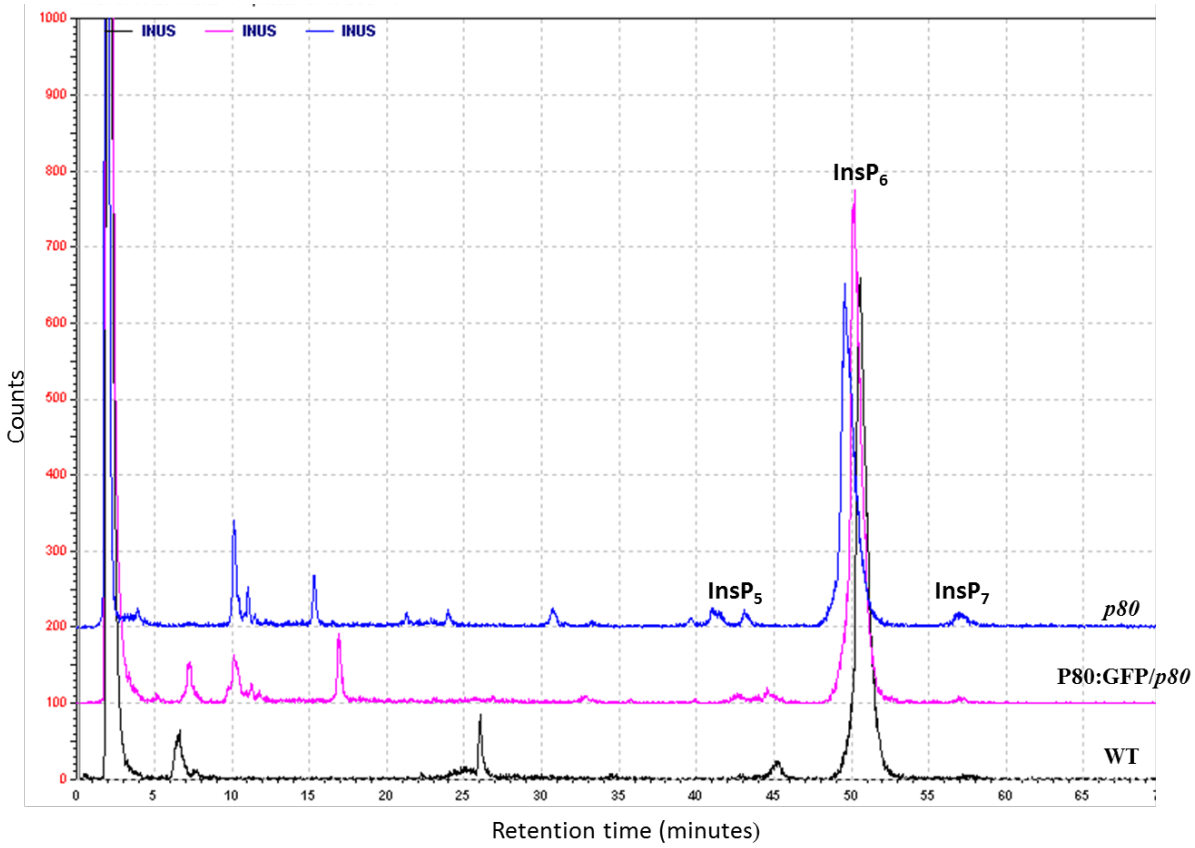

Figure 19: HPLC comparative trace analysis of InsPs in developing seeds of P80:GFP/*p80* with WT and *p80* mutants.

HPLC Trace comparative analysis of developing seeds of P80:GFP/*p80* (Pink trace) with wild-type (Black trace) and *p80* (Blue trace). $InsP_5$, $InsP_6$ and $InsP_7$ are indicated.

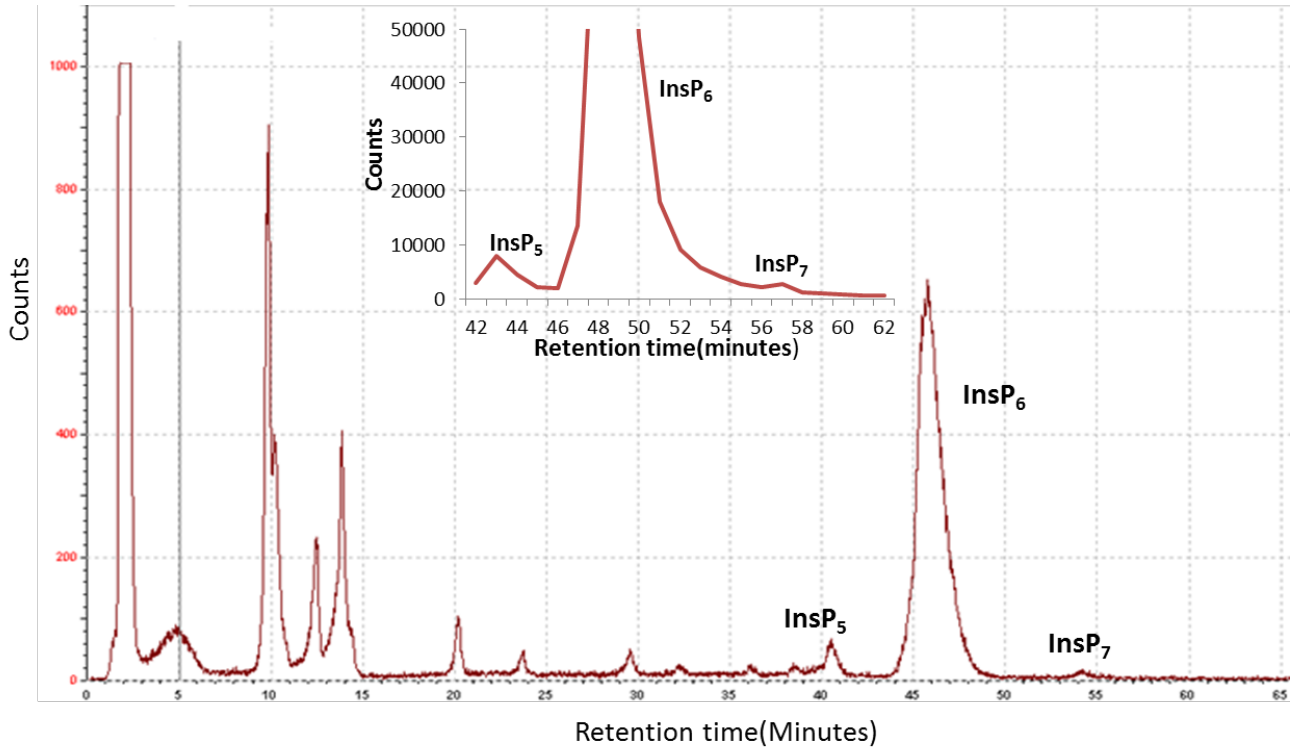

Figure 20: HPLC trace analysis of InsPs of *p80* mutant seedlings.

4 day-old mutant *p80* seedlings were radiolabelled with ^{3}H-*myo*-inositol, extracted and resolved using a Partisphere SAX anion exchange column. Distinct peaks for $InsP_5$ and $InsP_6$ were identified. A discrete peak for $InsP_7$ was also identified, novel for higher plants. **Inset:** Figure presents the scintillation counts of the trace. Fractions eluted from the HPLC are collected and analyzed independently using a scintillation counter.

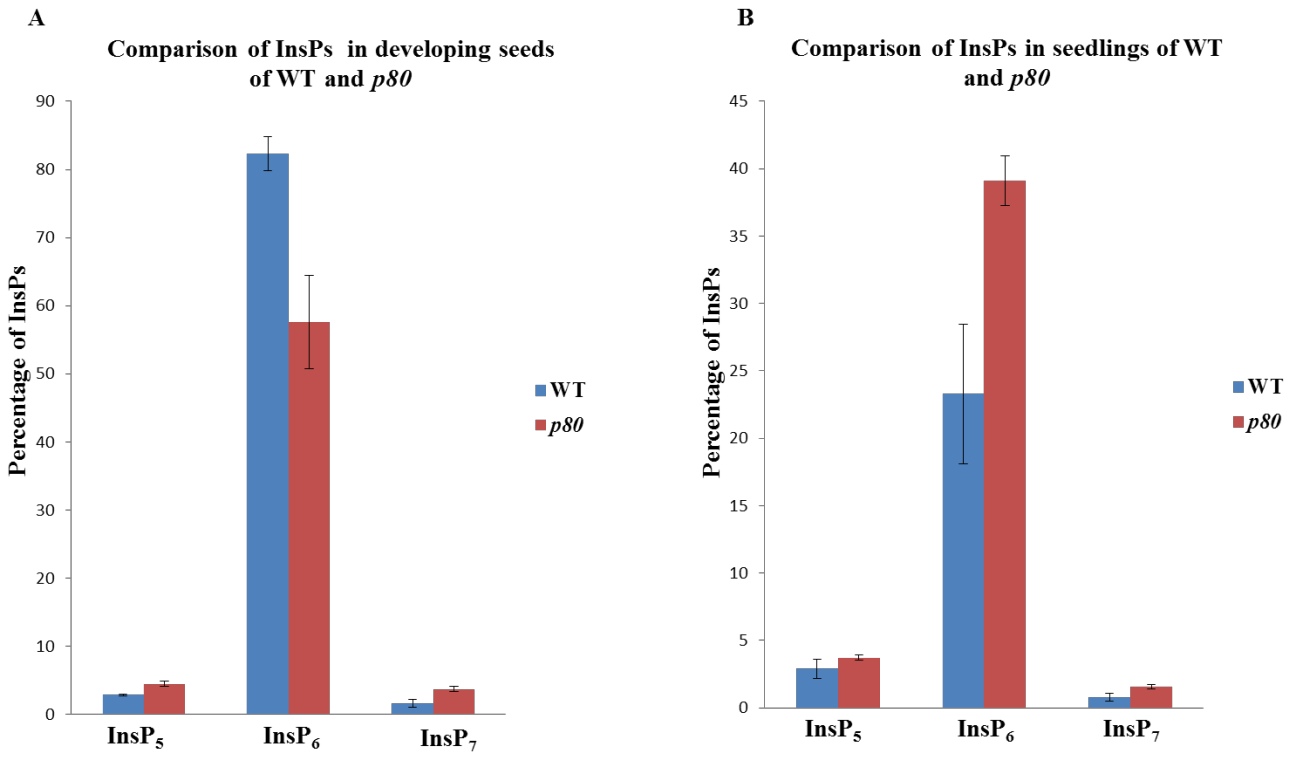

Figure 21: Comparison of amount of InsPs between wild-type and *p80* mutants.

The graphical figure presents a comparative analysis of the $InsP_5$, $InsP_6$ and $InsP_7$ in (A) siliques (p-value ≤ 0.01) and (B) seedlings (p-value ≤ 0.05). The error bars indicate standard deviation of the mean.

Inositol profiling of mutants deficient in $InsP_7$ synthesis enzymes

The genes involved in the biosynthesis of PPx-InsPs are called *VIP* genes and are conserved throughout eukaryotes, including higher plants. Plant species contain multiple expressed *VIP* genes that are 85% similar and 75% at the amino acid to the characterized animal *VIP*. Arabidopsis contains two highly conserved *VIP* genes, named *AtVIP1* and *AtVIP2*. The Gillaspy lab currently is analyzing two loss-of-function mutants of both *AtVIP1* (namely *vip1-1*, *vip1-2*) and *AtVIP2* (namely *vip2-1*, *vip2-2*).

The following data are the elution profile of InsPs of the *AtVIP2* mutant, *vip2-1*. The *vip2-1* seedlings were grown in 0.5x MS agar for 4 days, after which they were radiolabeled as described previously, extracted and separated using HPLC. Figure 20 shows the HPLC trace of *vip2-1* mutants overlaid with its wild-type seedlings trace. The mutants showed about 0.3% of $InsP_7$ of all InsPs. The amount of $InsP_6$ was calculated to be about 22.3%. These amounts were not significantly different from the corresponding age-matched WT grown under the same conditions. No significant change in the amounts of $InsP_5$ was detected between the wild-type and the *vip2-1* mutant seedlings.

We conclude that *vip2-1* does not vary significantly in the synthesis of $InsP_7$ as compared to its matched WT. This indicates that the $InsP_7$ synthesizing ability of the mutant was not reduced. It also showed very comparable amounts of $InsP_5$ and $InsP_6$ with the WT.

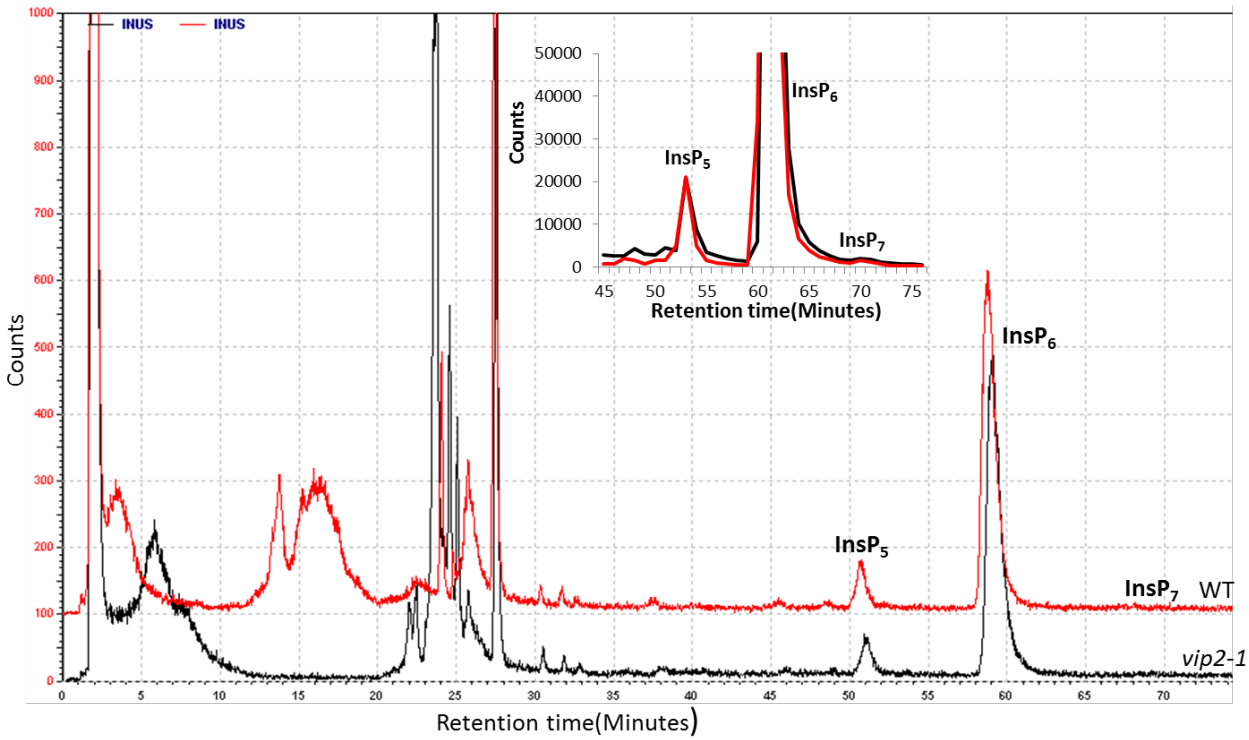

Figure 22: HPLC comparative trace analysis of InsPs of *vip2-1* mutant seedlings with wild-type seedlings.

HPLC trace comparative analysis of *vip2-1* mutant seedlings (Black trace) with wild-type seedlings (Red trace). $InsP_5$, $InsP_6$ and $InsP_7$ are indicated. **Inset** presents the scintillation count of the fractions of the indicated InsPs. Fractions eluted from the HPLC are collected and analyzed independently using a scintillation counter.

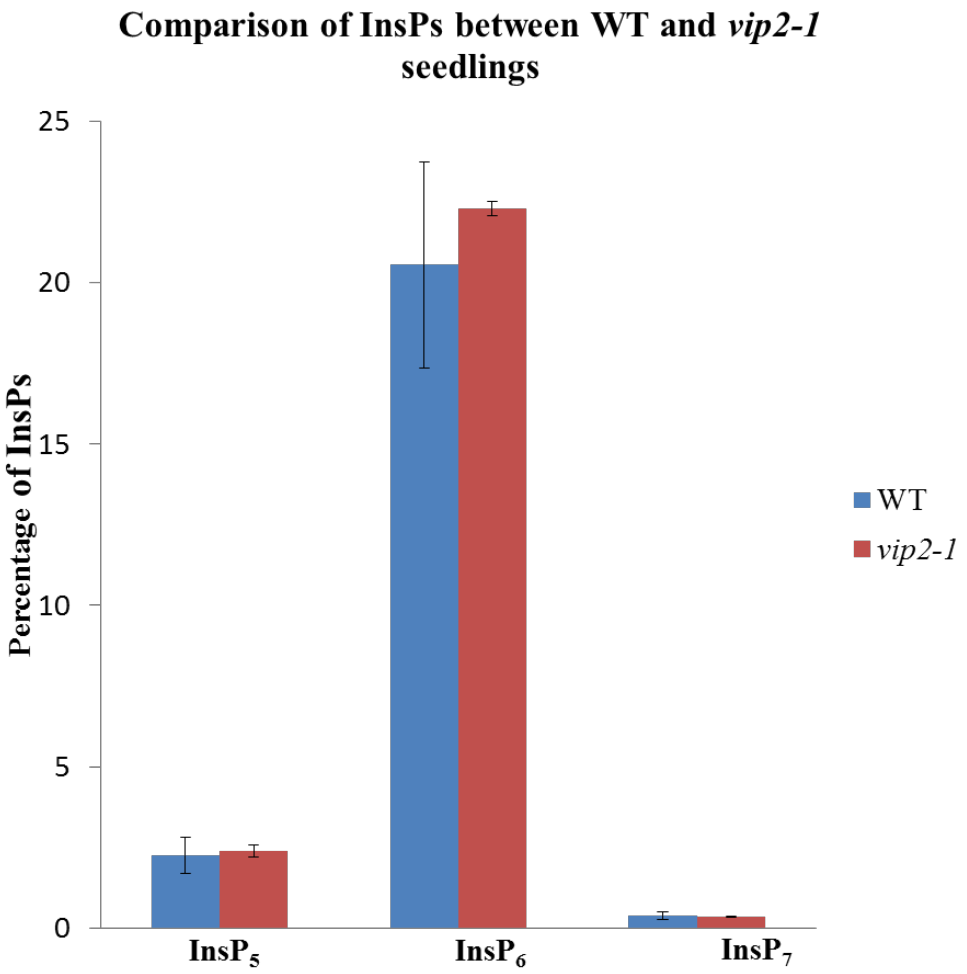

Figure 23: Comparison of amount of InsPs between wild-type and *vip2-1* mutants.

The figure presents a comparative analysis of the $InsP_5$, $InsP_6$ and $InsP_7$ in wild-type and *vip2-1* seedlings. The error bars indicate standard deviation of the mean.

DISCUSSION

Phytic acid, or $InsP_6$ is a well-known player in seed germination and viability. It is known to be an energy and phosphate source in seeds and aids in germination (Raboy 1997). $InsP_6$ serves as a precursor for a new class of inositol polyphosphates. These molecules contain pyrophosphate bonds and are emerging to be involved in various different biological processes. Review of literature shows that these unique molecules are involved in signaling in response to phosphate stress. Currently, only two reports in literature explore the presence of these PPx-InsPs in higher plants (Flores et al. 2000; Dorsch et al. 2003).

The work in this section was aimed to detect the occurrence of PPx-InsPs in plants. WT Arabidopsis vegetative tissue as well as developing seeds were examined. We radiolabelled the tissues and seed using ^{3}H-*myo*-Inositol and detected the incorporated InsPs using HPLC. We also analyzed the eluted fractions separately in a scintillation counter. Our results show the presence of $InsP_7$ in both seedlings and developing seeds. We also detected very high amount of $InsP_6$ in siliques. $InsP_6$ constituted of about 75% of all InsPs detected. This is congruous to previously reported data that $InsP_6$ is present in large amounts in seeds and functions during germination. The level of $InsP_6$ is reduced in seedlings and comprises of approximately 23% of all InsPs. Together, these data show that phytic acid is present in high quantities in germinating seeds and decreases with the development of the plant.

$InsP_7$, a unique PPx-InsP, was detected after the elution of $InsP_6$. We were able to calculate that $InsP_7$ makes up 2.6% of all InsPs in developing seeds as compared to 0.8% in seedlings. It can be speculated that these amounts correlate with the amount of $InsP_6$ present in the tissue. As the level of $InsP_6$ reduces, the synthesis of $InsP_7$ also decreases. We were not able to detect $InsP_8$ in either seedlings or developing seeds. $InsP_8$ may be present in lower quantities and may require a stronger and sensitive gradient of elution buffers to be detected.

We analyzed a mutant of *VIP2, vip2-1,* which is deficient in $InsP_7$ synthesis enzymes, along with its age-matched wild-type. This mutant has a T-DNA insertion between the tenth and the eleventh exon. Semi-quantitative analysis performed by our collaborator, Imara Perera, in North Carolina State University showed that no *VIP2* transcript was being made by this mutant, thereby presumably making no protein. We did not detect any significant changes in the levels of

InsPs between the WT and *vip2-1* mutant seedlings. The amount of $InsP_5$, $InsP_6$ and $InsP_7$ were similar to that of the WT seedlings. This suggests that even if the *VIP2* gene is disrupted, there may be other enzymes redundant in function to *At*VIP2, maintaining the production of $InsP_7$. This enzyme most likely is *At*VIP1. Interestingly, we noted that the amount of $InsP_7$ synthesized by these wild-type seedlings (obtained from North Carolina State University) were much lower, ~0.3%, than that synthesized by wild-type seedlings from our lab here at Virginia Tech, ~0.8%. This variability in $InsP_7$ levels could be attributed to differences in growth conditions like variable light, humidity or room temperature.

Arabidopsis P80 is predicted to play a role in a deubiquitination complex, thus taking part in the regulation of several different proteins. The loss-of-function mutant has a severe phenotype with growth and developmental retardation. Review of literature and studies of the amounts of different InsPs suggest that these mutants may have an alteration in their levels of InsPs, Our results indicate the *p80* mutants show a distinct variation in the level of inositol polyphosphates, especially $InsP_7$. In WT seedlings, $InsP_7$ constitutes of about 0.8% of all inositol polyphosphates. In comparison, *p80* mutant seedlings showed an increase, with $InsP_7$ constituting about 1.6% of all InsPs. $InsP_6$, the most common InsPs also showed a significant increase in the *p80* mutant, comprising of ~40% of all InsPs, in comparison to the wild-type synthesizing 23% $InsP_6$. The quantitative amount of $InsP_5$ was very comparable between the wild-type and the *p80* mutant in the seedlings, but differed significantly in developing seeds. Analysis of developing seeds of the *p80* mutant revealed some interesting results. We detected a marked decrease in the amount of $InsP_6$ as compared to the WT. In contrast, the synthesis of $InsP_7$ had increased by more than two times. This is intriguing in many ways. It can be hypothesized that the lower levels of $InsP_6$ may play a role in the unique distinct phenotypic appearance of the *p80* mutant. Also, it is very interesting to speculate that the loss-of-function of the *P80* gene confers stress upon the plant, thus resulting in the increase of $InsP_7$, communicating the signal to the plant.

CHAPTER IV

Objective 3. To examine the spatial expression pattern of the VIP kinases, *At*VIP1, *At*VIP2

INTRODUCTION

Ins is a simple polyol, which can be used as a building block on which both lipids and phosphates can be added (Gillaspy 2011). When phosphorylated, *myo*-inositol phosphates are critical signaling molecules, playing a role in different aspects of development, hormone signaling, vesicular trafficking, telomere maintenance and phosphate sensing and homeostasis (Boss et al. 2012). Previous studies have examined $InsP_3$, $InsP_4$, $InsP_5$, $InsP_6$ and their role as signaling molecules as well as storage molecules. $InsP_3$ acts as a signaling molecule, resulting in the release of Ca^{2+} from intracellular stores. It can also be phosphorylated to form more polar InsPs (Tsui et al. 2010). $InsP_4$ has been found to be a part of the histone acetylase complex, which controls condensation of chromatin. This ultimately affects gene regulation (Delage et al. 2013). $InsP_5$ and $InsP_6$ have been found to be cofactors for COI1 (coronatine insensitive 1), a jasmonic acid receptor (Mosblech et al. 2011) and TIR1 (Transport Inhibitor Response1), an auxin receptor (Tan et al. 2007) respectively. In these cases, the InsPs act as a molecular link in the E3 ubiquitin ligase pathway, thus controlling protein turnover. Phytic acid, or $InsP_6$ is a well-known player in seed germination and viability. Plants store high quantities of $InsP_6$ in seeds, to provide both an energy and phosphate source for the germinating seed (Raboy 1997). In addition, $InsP_6$ also chelates different cations (potassium, iron, zinc, magnesium) to form a salt, thus allowing the storage of these micronutrients in an inert form in the vacuole (Raboy 1997).

Recent data shows that there is a new class of InsPs containing pyrophosphate bonds on the Ins ring that have roles in sensing and signaling metabolic and abiotic stress (Bennett et al. 2006; Majerus 2007; Burton et al. 2009). There are two distinct sets of genes that have been shown to encode the enzymes that catalyze the synthesis of these PPx-InsPs. The first one, known as Inositol-hexakisphosphate kinase ($InsP_6K$) phosphorylate the 5-position on the Ins ring (Mulugu et al. 2007). No $InsP_6K$ genes have been found in Arabidopsis (Fassetti et al. 2011).

The second set, called the *VIP* genes, phosphorylates the 1- or the 3- position of the Ins ring (Mulugu et al. 2007). These genes are conserved throughout eukaryotes. They consist of two domains: an N-terminal ATP grasp domain that has kinase activity and a C-terminal histidine acid phosphatase domain. A BLAST search revealed that all plant species contain multiple *VIP* genes. The multiplicity of these expressed *VIP* genes in plants suggests that they use diverse ways to regulate the PPx-InsP levels in the cell. Arabidopsis contains two conserved *VIP* genes, *At*VIP1 (At3g01310) and *At*VIP2 (At5g15070). Our preliminary data indicate the differential expression of these genes in different tissues.

The VIP kinases, *At*VIP1 and *At*VIP2 kinases are proposed to catalyze the reaction from $InsP_6$ to form $InsP_7$ (Figure 24). My third objective is to determine where and when these genes are expressed. Examination of their unique expression patterns will help delineate how the PPx-InsPs are regulated in plants, thus leading towards their functional characterization.

Additionally, preliminary data from an independent yeast-two-hybrid screen carried out by our collaborators, the Perera lab from North Carolina State University, indicates that SnRK1.1 interacts with *At*VIP (unpublished data, not shown). This suggests a potential mechanism where SnRK1.1 phosphorylates VIP, possibly altering it to change PPx-InsP levels. Studies show that osmotic stress increases AMPK, the human counterpart of SnRK1.1, resulting in an increase in $1,5PP_2$-$InsP_4$ (Choi et al. 2008).

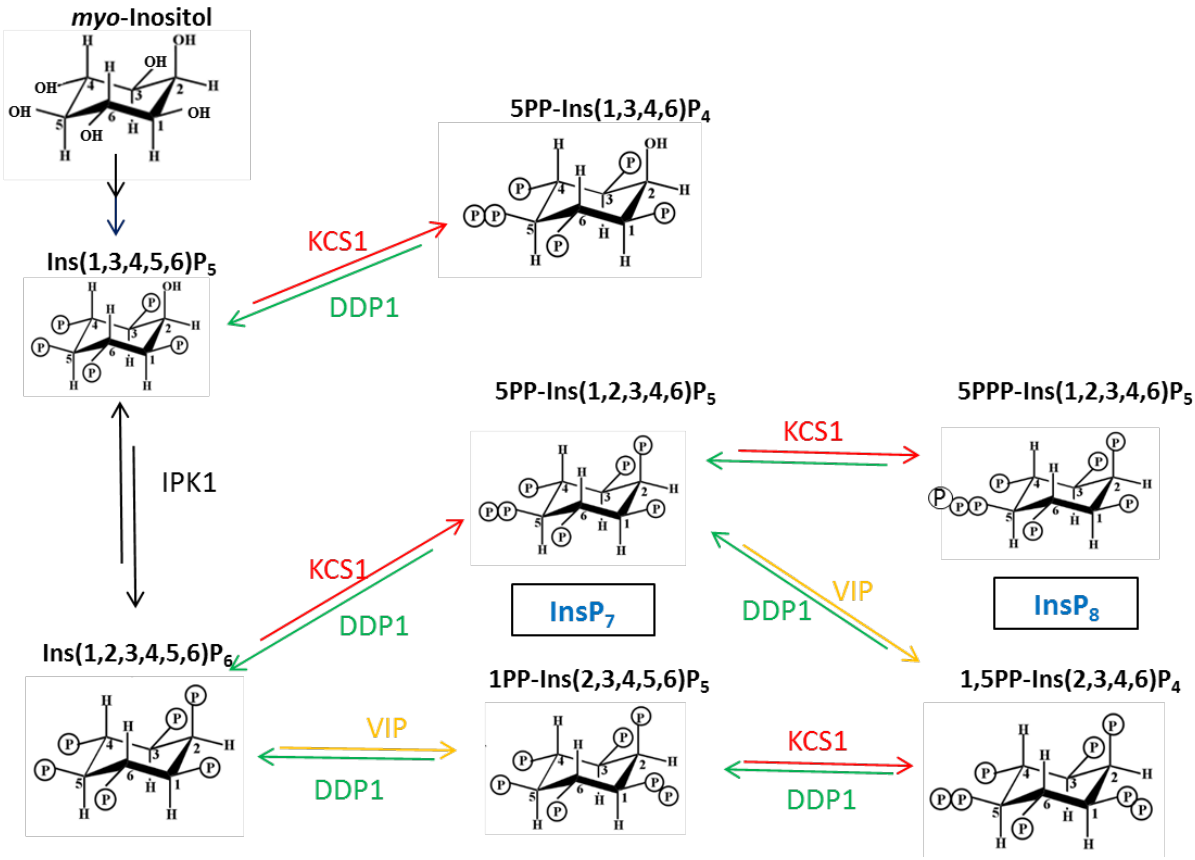

Figure 24: Pathway of PPx-InsPs synthesis.

The figure shows the final metabolic steps in $InsP_6$ synthesis in yeast. Red arrows show the activity of the kinases KCS1/$InsP_6K$, yellow arrows VIP kinase activity and the green arrows show the activity of a yeast phosphatase , Diphosphoinositol polyphosphate phosphohydrolase 1 (DDP1).

RESULTS

Structure of the promoter:GUS constructs

In order to characterize how the *VIP1* and *VIP2* genes are regulated *in vivo*, native VIP1 and VIP2 promoters were fused with the gene reporter, β-glucoronidase (GUS), and transformed into plants. The GUS system uses a histochemical reaction to monitor the expression pattern of the said gene. The enzyme removes glucoronic acid from the substrate 5-bromo-4-chloro-3-indolyl glucoronide (X-Gluc), to form 5, 5'-dibromo-4,4'-dichlor-indigo, a blue colored product (Jefferson 1989). The Korf lab software tool, IMEter v 2.0 (http://korflab.ucdavis.edu/cgi-bin/web-imeter2.pl) was used to determine the promoter sequences that affect expression of the gene (Parra et al. 2011). Using different databases, this software tool predicts different elements of promoter that will affect expression of the gene, and designate a numerical value. Based on this tool, primers were designed to amplify two sets of regions in *At*VIP1 and *At*VIP2. We included the entire intergenic region along with the 5' untranslated region (VIP1 and VIP2) for one round of amplification. For the second construct, we amplified the entire intergenic sequence, along with the 5' untranslated region, exon 1 and the first intron (VIP1Int and VIP2Int) as shown in Figure 25.

Of these two sets of constructs, the second set was used for creating the promoter: GUS constructs of the genes *At*VIP1, *At*VIP2 (Figure 26). These constructs were then transformed into Arabidopsis using the *Agrobacterium tumefaciens* transformation method (Bechtold N. 1993). We were able to generate several heterozygous lines and some homozygous lines for each gene, by screening for a linked BASTA resistance marker gene.

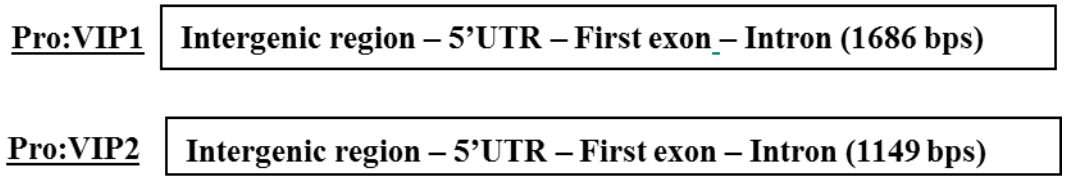

Figure 25: Regions amplified to build Promoter:GUS constructs.

The figure shows the regions of the genome amplified using PCR to build Promoter of gene fused to reporter gene, GUS for *At*VIP1 and *At*VIP2. The size of the regions amplified for VIP1 and VIP2 are 1686 bps and 1149 bps respectively.

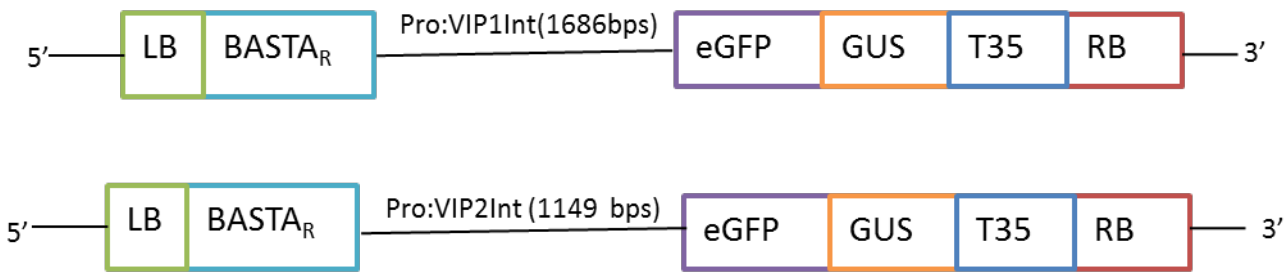

Figure 26: VIP1 and VIP2 Promoter:GUS constructs.

The figure shows VIP1 and VIP2 promoter GUS construct maps. Portions of each of the native promoters were fused to the green fluorescent protein (GFP) and GUS fusion transgene. This is followed by the 35S CaMV termination element (T35). Left border (LB) and Right border (RB) are indicated. The BASTA resistance gene ($BASTA_R$) allows for selection of transgenic plants.

Spatial expression pattern of *At*VIP1 Kinase

We wanted to determine the spatial pattern of *VIP1* and *VIP2* gene expression during development. For both these constructs we were able to obtain two independent, homozygous lines and several heterozygous. We confirmed the lines by genotyping and sequencing. Using VIP1p:GUS and VIP2p:GUS transgenic plants, we established spatial expression profiles based on GUS patterns from seedlings grown on agar plates containing 0.5x MS salts under regular light of 100-130 μE. We also examined the expression patterns in mature tissue of soil-grown plants.

Figure 27 shows the results from VIP1p:GUS plants. The expression of VIP1p:GUS is high in both vascular and non-vascular regions in the cotyledons. It is also to be noted that while the expression is more ubiquitous in cotyledons, it becomes more localized to vascular tissue in developed true leaves. GUS staining is very dark in newly developing true leaves. Expression can be observed in the vascular region in the root-shoot junction. The vascular nature of the promoter continued though the root. Expression was very high in the root tip (Figure 27D). We also observed intense staining in the lateral root primordial (Figure 27C). As with the primary root, the lateral root showed a vascular expression pattern also. No expression was detected in the trichomes (data not shown). Examination of the VIP1p:GUS expression patterns of mature plants grown in soil under 100-130 μE light was done. Expression of the *VIP1* gene promoter was detected in both cauline and rosette leaves. The promoter drives expression in the vascular regions of the leaf tissue as shown in Figure 27I. Expression was detected in sepals and some petals of flowers (Figure 27G and 27J). No GUS expression was detected in the stamens or the pistils. No promoter expression was observed in the developing seeds inside the seed pod (Figure 27F).

We conclude that VIP1p:GUS is expressed widely in seedlings, especially in the vascular tissue. It is also expressed in mature leaf tissue. The promoter of *VIP1* seems to be restricted in the flower, driving expression in petals and sepals, but not in the inner whorls (stamens and carpels). Expression was not very visible in the silique.

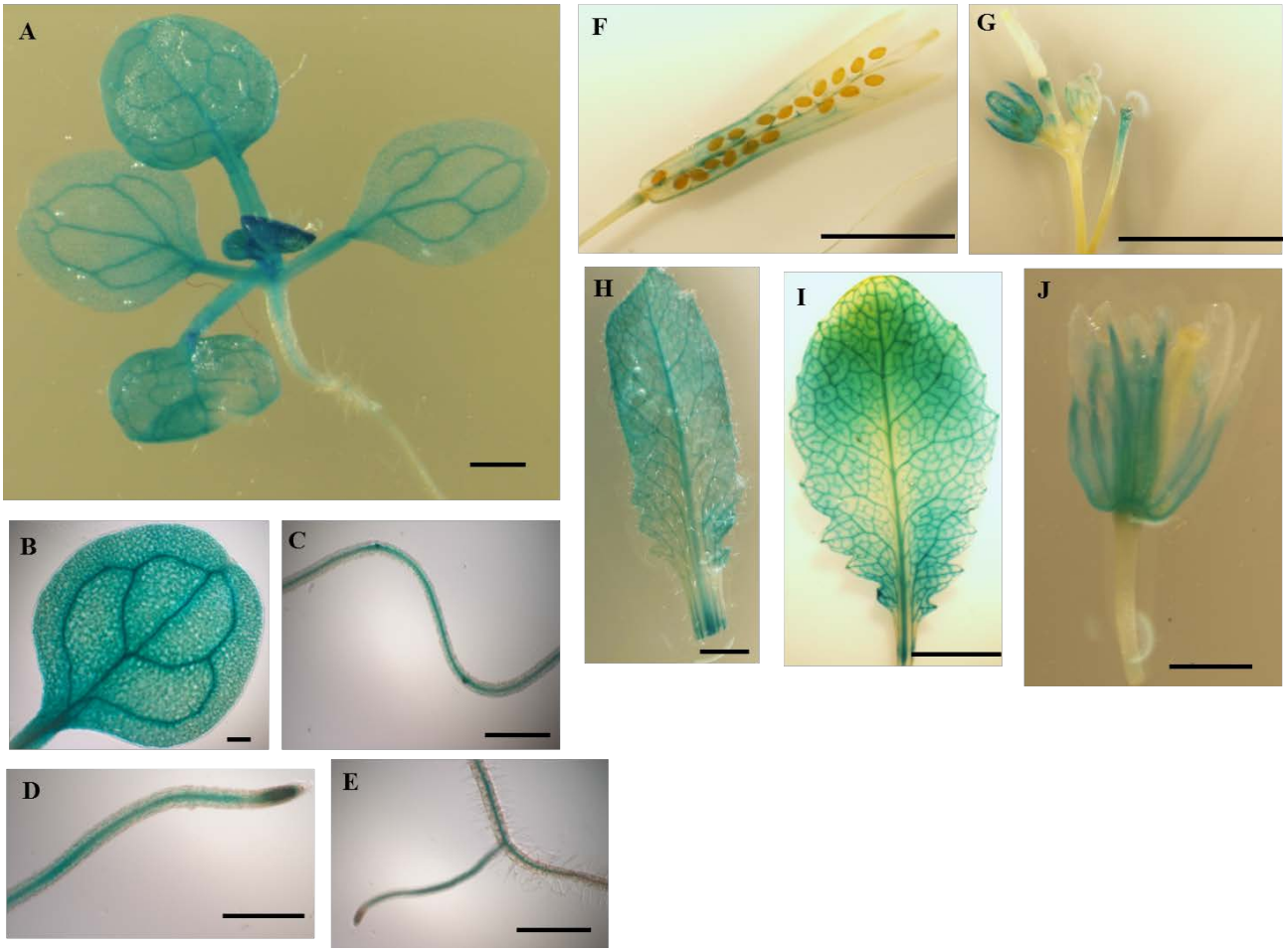

Figure 27: Spatial expression pattern of VIP1p:GUS in seedlings and mature tissue.

All seedlings were grown on 0.5x MS under regular light. A, B are 15 day-old seedlings and cotyledon. C, D, E are 10 day-old roots. H,I is mature rosette leaf, G, J are flowers, F is mature silique. Scale bars = 500 µm (A, C, E); 200 µm (D,B); 2 mm (F, G); 1 mm (H, I, J)

Spatial expression pattern of *At*VIP2 Kinase

Two homozygous lines of VIP2p:GUS and several heterozygous lines were generated. These lines were genotyped to confirm the presence of the construct in the transgenic plants. Seedlings were grown in 0.5x MS agar under regular light of 100-130 µE. Figure 28 shows the expression pattern of VIP2p:GUS in different tissues. Expression of the promoter was very strong in the seedling (Figure 28A). We were able to observe distinct vascular pattern in the cotyledons (Figure 28B) and true leaves. The VIP2 promoter was able to drive expression in the primary root (Figure 28D) and the lateral root (Figure 28F). We were able to detect expression in the lateral root primordial (Figure 28C). We were also able to detect expression of the promoter in the guard cells in the cotyledons (Figure 28E).

We examined the spatial expression patterns of mature soil-grown VIP2p:GUS plants. The promoter drove strong expression in the rosette leaves (Figure 28G). The vascular pattern was very distinct in the leaves. I was also able to observe expression of the promoter in flowers, mostly in the non-reproductive parts, sepals and petals (Figures 28H and 28I). Interestingly, a vascular pattern was evident in the petals as well. Expression of the promoter was observed in the developing seeds in the siliques and in the pedicel (Figure 28J).

We conclude that *VIP2* promoter is expressed in most tissues, in shoots and roots. It is expressed in the flowers, although not much expression was detected in the stamens. Microarray data from eFP browser and Genevestigator predicts high expression in the stamens. We detected expression in the developing siliques, which was unique to *VIP2*.

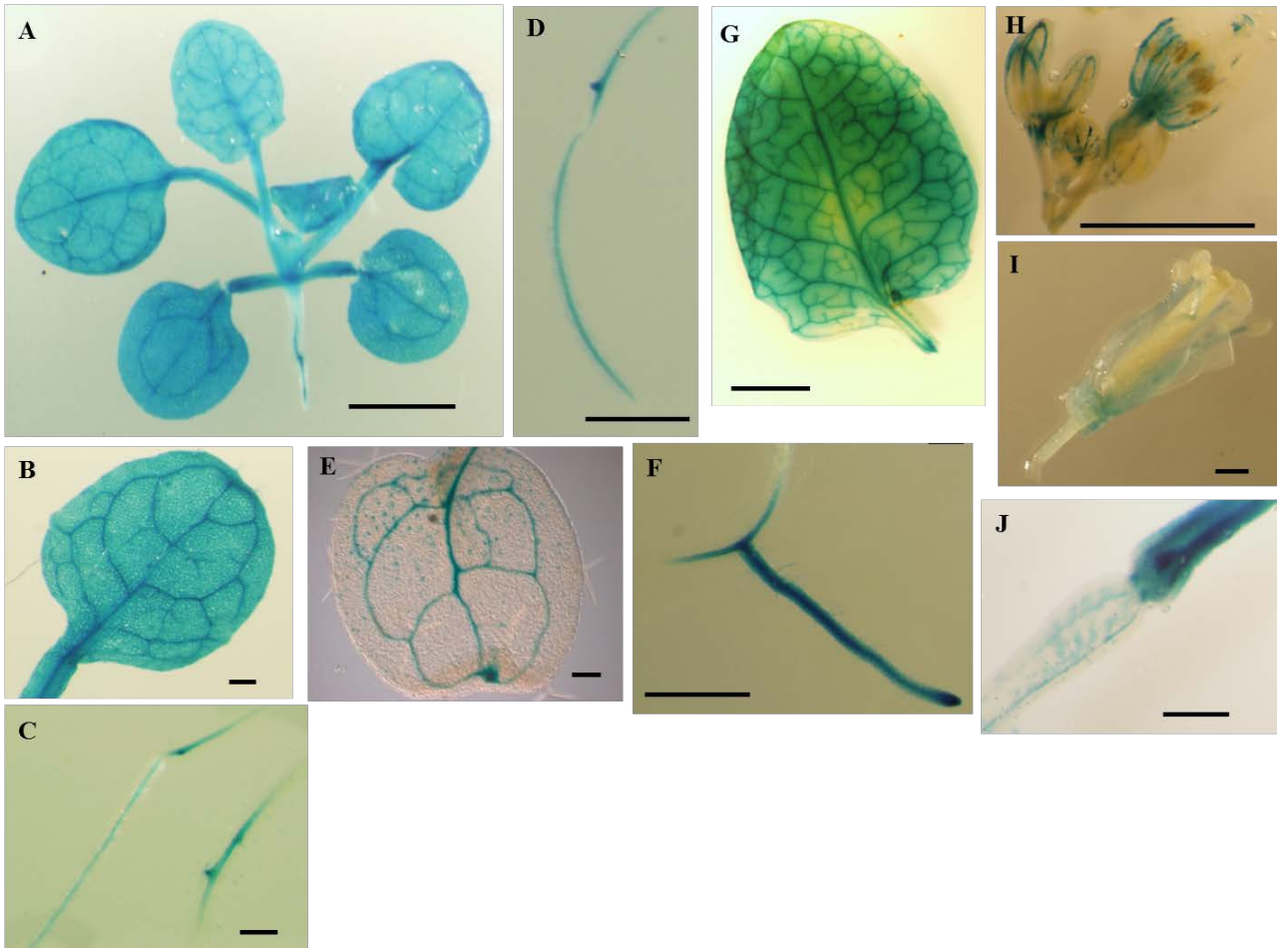

Figure 28: Spatial expression pattern of VIP2p:GUS in seedlings and mature tissue.

All seedlings were grown on 0.5x MS under regular light of 100-130 µE. A and B are 15-day old seedlings and cotyledon. E is 10 day-old cotyledon. C, D and F are 10 day-old roots. G is mature rosette leaf, H and I are flowers, J is a silique. Scale bars = 2 mm (A, G); 200 µm (B,E); 500 µm (D, F); 1 mm (C, H, I, J).

DISCUSSION

The proposed enzymes that are involved in the synthesis of PPx-Ins are VIP kinases. The VIP kinases, *At*VIP1 and *At*VIP2 kinases have been predicted to catalyze the reaction to form $InsP_7$ from $InsP_{6.}$ Determining where and when these genes are expressed, examining their unique expression patterns will help delineate how the PPx-InsPs are regulated in plants. This will help to characterize them functionally.

In this section, we have elucidated the spatial expression patterns of the two VIP kinases, *At*VIP1 and *At*VIP2. Expression of VIP1 was observed in seedlings. The vascular pattern was depicted in cotyledons as well as mature leaf tissues. The promoter VIP1 drove expression of the reporter gene in primary root, lateral roots and lateral root primordia. We did not detect any expression in the seeds. We were able to detect expression in flowers but not in the reproductive organs. Microarray data analysis from Arabidopsis eFP browser predicts the expression of the *VIP1* gene in all tissues, with lowest level in mature pollen. Interestingly, *VIP2* gene is predicted to have minimal expression in most tissues, suggesting that VIP1 is the key enzyme in the synthesis of PPx-InsPs. My results from the PromoterVIP2:GUS do not support this data. We detected expression of the gene in most tissues, including developing seeds. The expression was vascular in several tissues. Preliminary qRT-PCR analysis performed by our collaborator has shown differential expression of VIP2 in various tissues. Microarray data predicts high levels of VIP2 in mature pollen. More analysis on the different developmental stages of the flowers will help to establish this.

CHAPTER V

FUTURE DIRECTIONS

My research was based on exploring the role that the *Arabidopsis thaliana* protein P80 plays in the plant system. Characterization of the phenotype of the loss-of-function *p80* mutant shows that this protein plays an important part in the plant biology. My preliminary results show the absence of P80 may result in decreased transcript of SnRK1.1:GFP. This may be the cause of improper localization and possibly destabilization of SnRK1.1. This indicates that P80 is involved in the regulation of the energy sensor, SnRK1.1. The delineation of the exact mechanism by which this regulatory process occurs remains to be elucidated. Also, I would like to characterize the alternate splice variant of SnRK1.1 in the *p80* mutant background. This variant is comprised of 512 AA, as compared to the 535 AA in the variant that was analyzed in this work. I would like to investigate if this splice variant interacts with P80 directly. It will be very intriguing to note the subcellular localization and protein stability of this truncated SnRK1.1 and compare it to its expression in the *p80* mutant background.

Furthermore, my results also show that P80 may not be involved in the regulation of SnRK1.2. It will be very interesting to study the role of SnRK1.2 in the cell and its regulation. It is homologous to SnRK1.1, but no data in literature has shown redundancy of function. SnRK1.2p:GUS spatial expression patterns as well as the overexpression of SnRK1.2:GFP in the WT background do not show any evidence of redundancy with SnRK1.1 either. I would like to characterize the phenotypes exhibited by the lines overexpressing SnRK1.2:GFP, to elucidate the importance of SnRK1.2 in plants.

Mutants in P80 also show an alteration in the amount of PPx-InsPs produced as compared to the wild-type. I would like to study the involvement of P80 in the alteration of PPx-InsPs like $InsP_7$ and $InsP_8$. Using HPLC, I showed the presence of $InsP_7$ in both vegetative tissue and developing seeds of *Arabidopsis thaliana*. I was not able to detect $InsP_8$. Flores et al. 2006 showed the presence of $InsP_8$ in Duckweed, *Spirodela polyrrhiza.* Altering the elution gradient may help in detection of $InsP_8$. I elucidated the expression patterns of the two enzymes involved in the synthesis of $InsP_7$ and $InsP_8$. Microarray data and preliminary analysis of these enzymes

show that they are stimulated by low phosphate. I would like further characterize the spatial patterns, in response to stresses like phosphate. Expression changes in response to other nutrients, like carbon, and light will be very interesting to observe and informative about these enzymes and thereby, about their regulation and synthesis of PPx-InsPs. I would also like to confirm and quantify the spatial expression pattern using qRT-PCR. Mutant analysis and functional characterization of VIP1 and VIP2 is being carried out by members of the Gillaspy and the Perera labs.

CHAPTER VI

MATERIALS AND METHODS

Plant growth conditions:

Arabidopsis thaliana ecotype Columbia (Col) was used for all the experiments. Plants were grown in a controlled growth chamber, maintained at a temperature of 22-24^{o}C and humidity of ~35%. Visible light of 100-130 µE was provided for 16 hours/day (long-day conditions). All plants were grown using Sunshine#1 soil mix and fertilized with MiracleGro Liquid Houseplant Food (Composition - 8% total nitrogen, 7% available phosphate, P_2O_5, 6% soluble potash). For plate-grown seedlings analyses, all seeds were sterilized using 30% Clorox and rinsed with sterile water. The seeds were germinated on 0.5x Murashige and Skoog Basal salts ± 1% or 3% Sucrose. Seeds on plates as well as in pots were stratified at 4^{o}C for 3 days before being transferred to the growth chamber.

Sub-cellular Localization:

The coding regions of SnRK1.1 and SnRK1.2 were amplified using high-fidelity PCR (Velocity enzyme, Bio-Rad Laboratories, Hercules, CA), confirmed using sequencing and then cloned into the pENTR/D-TOPO vector (Invitrogen). This was recombined into pK7FWG2 using the Gateway cloning system according to the manufacturer's instructions. The resulting construct, with the 35S Cauliflower Mosaic virus promoter followed by the SnRK1.1:GFP or the SnRK1.2:GFP was transformed into *Agrobacterium tumefaciens* as described (Clough et al. 1998; Karimi et al. 2002). SnRK1.1:GFP or SnRK1.2:GFP in wild-type or *p80* were identified using the selection marker, kanamycin. Independent homozygous lines were selected for each construct and used for analyses of subcellular localization. Seedlings were harvested at 4 and 11 days and used for GFP fluorescence detection using Zeiss LSM 510 laser scanning microscope (Carl Zeiss) with an inverted Axio Observer Z1 base. Excitation was done using a 488-nm argon laser and fluorescence detected using 505- to 550-nm band-pass emission filter. Slides were examined with x40 C-Apochromat water immersion lens.

qRT-PCR:

RNA extraction- Total RNA was extracted from 100 mg of frozen tissue using RNeasy Plant Mini kit (Qiagen, Valencia, CA). RNA was measured using a NanoDrop ND-1000 Spectrophotometer (Thermo Scientific Nanodrop Technologies, LLc, Wilmington, DE).

cDNA synthesis- Up to one microgram of total RNA was reverse transcribed using the iScript cDNA Synthesis Kit according to the manufacturer's instructions (Bio-Rad laboratories, Hercules, CA). The resulting cDNA was used as a template in each PCR reaction.

Quantitative PCR- Quantitative PCR was performed using SYBR GREEN reagent (Applied Biosystems, Foster city, CA). Each reaction was carried out in triplicates and was monitored using the Applied Biosystems 7300 Real-Time PCR instrumentation (Applied Biosystems, Foster city, CA). C_t values of Peroxisomal Ubiquitin 4, PEX4, used as an endogenous control, were compared with the sample C_t values. Inverse logarithms were applied to determine relative changes in expression (Donahue et al. 2010).

Western Blotting:

Plant extracts- All plant tissues were frozen in liquid nitrogen and ground using a mortar and pestle. The finely ground powder was homogenized in an extraction buffer (50 mM Tris, pH 7.5, 150 mM NaCl, 5mM $MgCl_2$ and 0.05% TritonX 100). A protease inhibitor cocktail, P9599, from Sigma Aldrich was also added to the extraction buffer. The homogenized sample was centrifuged at 13200 rpm for 2 minutes in a table-top microcentrifuge. The supernatant was mixed with protein loading buffer (100mM Tris, pH 6.8, 4% Sodium Dodecyl Sulphate, 0.2% Bromophenol blue and 20% Glycerol, 14μL/mL β-mercaptoethanol). The samples were boiled for 10 minutes, centrifuged and the supernatants were used for Western Blot analyses.

Western Blots - Proteins were electrophoresed using 10% SDS-PAGE and then transferred to a nitrocellulose membrane using a semi-dry transfer system apparatus (BioRad laboratories, Hercules, CA). After detecting total protein on the membrane using Ponceau S staining (Gallagher et al. 2001; Blancher et al. 2012), the nitrocellulose membrane was blocked using 5% non-fat milk in deionized water for 3 hours at room temperature. For detection of the GFP-tagged proteins, anti-GFP antibody from (Rockland Immunochemicals Inc.) was used at a dilution of 1:5000. The native SnRK1 proteins were detected using anti-SnRK1 antibody (Jenna Hess, Cocalico Biologicals Inc., PA). All antibodies were used in 2.5% Non-fat milk in

deionized water solutions. The membrane was incubated with primary antibody overnight at 4^{o}C. The membranes were probed with 1:2000 dilution of goat anti-rabbit horseradish peroxidase after washing three times with 1X TBST (50 mM Tris-HCl, pH 7.5, 0.9% NaCl, 0.01% Tween-20). Membranes were activated using Amersham ECL Prime Western Blotting Detection Reagent from GE Healthcare, UK and signals detected after exposing to x-ray.

High Pressure Liquid Chromatography:

Sample collection: For analysis of developing seeds, green siliques of similar developmental stage were chosen, clipped with the pedicel. 6-8 siliques were selected for each labeling experiment run. For seedling analysis, ~15 4-day old seedlings were collected from 0.5x MS plates that were placed in the growth chamber after three days of stratification at 4^{o}C (Stevenson-Paulik et al. 2006).

Radiolabeling- The samples were placed in an eppendorf tube with 50µl of 1x MS + 1% sucrose solution (pH 5.7). 100 µl (100 mCuries/ml) of ^{3}H-*myo*-inositol (American Radiolabeled Chemicals, St.Louis, MO) was added to each tube. The tubes were kept under light for 4 days.

Extraction- The extraction of InsPs was done as per the protocol described in Azevedo et al. (Azevedo 2006). Briefly, samples were grounded in extraction buffer (25mM EDTA, 10mg/ml $InsP_6$ and 1M Perchloric acid ($HClO_4$). Glass beads were added and the samples were vortexed. The supernatants were obtained and neutralized until the pH is between 6 and 8 using the neutralization buffer (250 mM EDTA, 1M K_2CO_3). Carbon-dioxide is allowed to diffuse properly after which the samples were dry-extracted until the volume became about 70µl.

HPLC Run and Analysis- Binary HPLC pump (Beckman Coulter) equipped with partisphere SAX 4.6 X 125 mm column and connected through a guard cartridge was used. Elution gradient for HPLC was set up as per Azevedo et al using Buffer A (1mM EDTA) and Buffer B (1.3M Ammonium Phosphate, pH 3.8). The flow rate was set to 1ml/min. 4ml of Ultima-Flo AP scintillation cocktail (Perkin Elmer, Waltham, MA) was added to each fraction to quantify the radioactivity of the eluted fractions using IN/US radiation detector.

Normalization of InsPs- All calculations were done using the data obtained from the scintillation counter. The ^{3}H-*myo*-Ins incorporated in InsPs was calculated by taking the sum of all counts and subtracting the ^{3}H-Ins peak count. This was termed Total InsPs. The amount of each InsP was calculated as follows:
[(Σ CPMs found in peak) / (Total InsPs)]*100]

Promoter analyses:

The Korf lab software tool, IMEter v 2.0 http://korflab.ucdavis.edu/cgi-bin/web-imeter2.pl, (Parra et al. 2011) was used to determine the promoter sequences that affect expression of the gene.

GUS Detection:

Samples of 4 and 10 day-old seedlings grown on 0.5x MS media and mature plant tissues were used for GUS assay. The samples were immersed in the GUS solution (0.025 µM ferrocyanide, 0.025 µM ferrous cyanide, 0.1 mM sodium phosphate buffer pH 7.0, 0.01% Triton X-100, 0.5 µg/mL 5-bromo-4-chloro-3-indoyl-β-D-glucuronic acid), vacuum–infiltrated for 15-20 minutes at 17.5 mTorr and incubated at 37^{o}C overnight (Styer et al. 2004). The sample solution was removed, replaced with 70% ethanol and incubated at 4^{o}C for 2-3 hours. The 70% ethanol was replaced with 99% ethanol. Samples were imaged using Olympus SZX16 microscope.

REFERENCES

Alderson, A., P. A. Sabelli, J. R. Dickinson, D. Cole, M. Richardson, M. Kreis, P. R. Shewry and N. G. Halford (1991). "Complementation of *snf1*, a mutation affecting global regulation of carbon metabolism in yeast, by a plant protein kinase cDNA." Proceedings of the National Academy of Sciences **88**(19): 8602-8605.

Ananieva, E. A., G. E. Gillaspy, A. Ely, R. N. Burnette and F. L. Erickson (2008). "Interaction of the WD40 Domain of a Myoinositol Polyphosphate 5-Phosphatase with SnRK1 Links Inositol, Sugar, and Stress Signaling." Plant Physiology **148**(4): 1868-1882.

Azevedo, C., Saiardi, Adolfo (2006). "Extraction and analysis of soluble inositol polyphosphates from yeast." Nature Protocols **1**(5): 1754-2189.

Baena-Gonzalez, E., F. Rolland, J. M. Thevelein and J. Sheen (2007). "A central integrator of transcription networks in plant stress and energy signalling." Nature **448**(7156): 938-942.

Bechtold N., E. J., Pelletier G. (1993). "Agrobacterium mediated in planta gene transfer by infiltration of adult *Arabidopsis thaliana* plants = plants in planta transformation of adult *Arabidopsis thaliana* by Agrobacterium infiltration." Proceedings of the Academy of Sciences. Series 3 Life Science **316**.

Bennett, M., S. M. N. Onnebo, C. Azevedo and A. Saiardi (2006). "Inositol pyrophosphates: metabolism and signaling." Cellular and Molecular Life Sciences **63**(5): 552-564.

Berdy, S. E., J. Kudla, W. Gruissem and G. E. Gillaspy (2001). "Molecular Characterization of At5PTase1, an Inositol Phosphatase Capable of Terminating Inositol Trisphosphate Signaling." Plant Physiology **126**(2): 801-810.

Blancher, C. and R. Cormick (2012). Sodium Dodecyl Sulphate–Polyacrylamide Denaturing Gel Electrophoresis and Western Blotting Techniques. Metastasis Research Protocols. M. Dwek, S. A. Brooks and U. Schumacher, Humana Press. **878:** 89-110.

Boer, V. M., C. A. Crutchfield, P. H. Bradley, D. Botstein and J. D. Rabinowitz (2010). "Growth-limiting Intracellular Metabolites in Yeast Growing under Diverse Nutrient Limitations." Molecular Biology of the Cell **21**(1): 198-211.

Boss, W. F. and Y. J. Im (2012). "Phosphoinositide Signaling." Annual Review of Plant Biology **63**(1): 409-429.

Bradford, M. M. (1976). "A rapid and sensitive method for the quantitation of microgram quantities of protein utilizing the principle of protein-dye binding." Analytical Biochemistry **72**(1–2): 248-254.

Burton, A., X. Hu and A. Saiardi (2009). "Are inositol pyrophosphates signalling molecules?" Journal of Cellular Physiology **220**(1): 8-15.

Chen, X., W.-H. Lin, Y. Wang, S. Luan and H.-W. Xue (2008). "An Inositol Polyphosphate 5-Phosphatase Functions in PHOTOTROPIN1 Signaling in Arabidopis by Altering Cytosolic Ca^{2+}." The Plant Cell **20**(2): 353-366.

Cho, Y. H., J. W. Hong, E. C. Kim and S. D. Yoo (2012). "Regulatory functions of SnRK1 in stress-responsive gene expression and in plant growth and development." Plant Physiology **158**(4): 1955-1964.

Choi, K., E. Mollapour, J. H. Choi and S. B. Shears (2008). "Cellular Energetic Status Supervises the Synthesis of Bis-Diphosphoinositol Tetrakisphosphate Independently of AMP-Activated Protein Kinase." Molecular Pharmacology **74**(2): 527-536.

Clough, S. J. and A. F. Bent (1998). "Floral dip: a simplified method forAgrobacterium-mediated transformation of *Arabidopsis thaliana*." The Plant Journal **16**(6): 735-743.

Cohn, M. A., Y. Kee, W. Haas, S. P. Gygi and A. D. D'Andrea (2009). "UAF1 Is a Subunit of Multiple Deubiquitinating Enzyme Complexes." Journal of Biological Chemistry **284**(8): 5343-5351.

Cohn, M. A., P. Kowal, K. Yang, W. Haas, T. T. Huang, S. P. Gygi and A. D. D'Andrea (2007). "A UAF1-Containing Multisubunit Protein Complex Regulates the Fanconi Anemia Pathway." Molecular Cell **28**(5): 786-797.

Delage, E., J. Puyaubert, A. Zachowski and E. Ruelland (2013). "Signal transduction pathways involving phosphatidylinositol 4-phosphate and phosphatidylinositol 4,5-bisphosphate: Convergences and divergences among eukaryotic kingdoms." Progress in Lipid Research **52**(1): 1-14.

Doelling, J. H., A. R. Phillips, G. Soyler-Ogretim, J. Wise, J. Chandler, J. Callis, M. S. Otegui and R. D. Vierstra (2007). "The Ubiquitin-Specific Protease Subfamily UBP3/UBP4 Is Essential for Pollen Development and Transmission in Arabidopsis." Plant Physiology **145**(3): 801-813.

Donahue, J. L., S. R. Alford, J. Torabinejad, R. E. Kerwin, A. Nourbakhsh, W. K. Ray, M. Hernick, X. Huang, B. M. Lyons, P. P. Hein and G. E. Gillaspy (2010). "The *Arabidopsis thaliana myo*-inositol 1-phosphate synthase1 gene is required for *myo*-inositol synthesis and suppression of cell death." The Plant Cell **22**(3): 888-903.

Dorsch, J. A., A. Cook, K. A. Young, J. M. Anderson, A. T. Bauman, C. J. Volkmann, P. P. N. Murthy and V. Raboy (2003). "Seed phosphorus and inositol phosphate phenotype of barley low phytic acid genotypes." Phytochemistry **62**(5): 691-706.

Ercetin, M., E. Ananieva, N. Safaee, J. Torabinejad, J. Robinson and G. Gillaspy (2008). "A phosphatidylinositol phosphate-specific *myo*-inositol polyphosphate 5-phosphatase required for seedling growth." Plant Molecular Biology **67**(4): 375-388.

Fassetti, F., O. Leone, L. Palopoli, S. Rombo and A. Saiardi (2011). "IP_6K gene identification in plant genomes by tag searching." BMC Proceedings **5**(Suppl 2): S1.

Flores, S. and C. C. Smart (2000). "Abscisic acid-induced changes in inositol metabolism in *Spirodela polyrrhiza*." Planta **211**(6): 823-832.

Gallagher, S., S. E. Winston, S. A. Fuller and J. G. R. Hurrell (2001). Immunoblotting and Immunodetection. Current Protocols in Immunology, John Wiley & Sons, Inc.

Garcia-Santisteban, I., K. Zorroza and J. A. Rodriguez (2012). "Two Nuclear Localization Signals in USP1 Mediate Nuclear Import of the USP1/UAF1 Complex." PloS one **7**(6): e38570.

Ghillebert, R., E. Swinnen, J. Wen, L. Vandesteene, M. Ramon, K. Norga, F. Rolland and J. Winderickx (2011). "The AMPK/SNF1/SnRK1 fuel gauge and energy regulator: structure, function and regulation." FEBS Journal **278**(21): 3978-3990.

Gillaspy, G. E. (2011). "The cellular language of *myo*-inositol signaling." New Phytologist **192**(4): 823-839.

Gunesekera, B., J. Torabinejad, J. Robinson and G. E. Gillaspy (2007). "Inositol Polyphosphate 5-Phosphatases 1 and 2 Are Required for Regulating Seedling Growth." Plant physiology **143**(3): 1408-1417.

Halford, N. G., Hey, Sandra J. (2009). "Snf1-related protein kinases (SnRKs) act within an intricate network that links metabolic and stress signalling in plants " Biochemical Journal **419**(2): 247-259.

Hardie, D. G. (2007). "AMPK and SNF1: Snuffing Out Stress." Cell metabolism **6**(5): 339-340.

Hardie, D. G. (2008). "AMPK: a key regulator of energy balance in the single cell and the whole organism." Int J Obes **32**(s4).

Hardie, D. G. (2011). "AMP-activated protein kinase—an energy sensor that regulates all aspects of cell function." Genes & Development **25**(18): 1895-1908.

Imai, S., M. Kano, K. Nonoyama and S. Ebihara (2013). "Behavioral Characteristics of Ubiquitin-Specific Peptidase 46-Deficient Mice." PloS one **8**(3): e58566.

Jefferson, R. A. (1989). "The GUS reporter gene system." Nature **342**(6251): 837-838.

Kane, P. M. and K. J. Parra (2000). "Assembly and regulation of the yeast vacuolar H(+)-ATPase." J Exp Biol **203**(Pt 1): 81-87.

Karimi, M., D. Inzé and A. Depicker (2002). "GATEWAY™ vectors for Agrobacterium-mediated plant transformation." Trends in plant science **7**(5): 193-195.

Kaye, Y., Y. Golani, Y. Singer, Y. Leshem, G. Cohen, M. Ercetin, G. Gillaspy and A. Levine (2011). "Inositol Polyphosphate 5-Phosphatase7 Regulates the Production of Reactive Oxygen Species and Salt Tolerance in Arabidopsis." Plant Physiology **157**(1): 229-241.

Kee, Y., K. Yang, M. A. Cohn, W. Haas, S. P. Gygi and A. D. D'Andrea (2010). "WDR20 Regulates Activity of the USP12·UAF1 Deubiquitinating Enzyme Complex." Journal of Biological Chemistry **285**(15): 11252-11257.

Kelley L.A, S. M. J. E. (2009). "Protein structure prediction on the web: a case study using the Phyre server." Nature Protocols(4): 363 - 371.

Krinke, O., Z. Novotná, O. Valentová and J. Martinec (2007). "Inositol trisphosphate receptor in higher plants: is it real?" Journal of Experimental Botany **58**(3): 361-376.

Lee, Y.-S., S. Mulugu, J. D. York and E. K. O'Shea (2007). "Regulation of a Cyclin-CDK-CDK Inhibitor Complex by Inositol Pyrophosphates." Science **316**(5821): 109-112.

Li, D. and R. Roberts (2001). "Human Genome and Diseases: WD-repeat proteins: structure characteristics, biological function, and their involvement in human diseases." Cellular and Molecular Life Sciences CMLS **58**(14): 2085-2097.

Lin, W.-H., Y. Wang, B. Mueller-Roeber, C. A. Brearley, Z.-H. Xu and H.-W. Xue (2005). "*At*5PTase13 Modulates Cotyledon Vein Development through Regulating Auxin Homeostasis." Plant Physiology **139**(4): 1677-1691.

Liu, T.-Y., C.-Y. Chang and T.-J. Chiou (2009). "The long-distance signaling of mineral macronutrients." Current Opinion in Plant Biology **12**(3): 312-319.

Luo, H. R., Y. E. Huang, J. C. Chen, A. Saiardi, M. Iijima, K. Ye, Y. Huang, E. Nagata, P. Devreotes and S. H. Snyder (2003). "Inositol Pyrophosphates Mediate Chemotaxis in Dictyostelium via Pleckstrin Homology Domain-PtdIns(3,4,5)P_3 Interactions." Cell **114**(5): 559-572.

Majerus, P. W. (2007). "A Discrete Signaling Function for an Inositol Pyrophosphate." Sci. STKE **2007**(416): pe72-.

McKibbin, R. S., N. Muttucumaru, M. J. Paul, S. J. Powers, M. M. Burrell, S. Coates, P. C. Purcell, A. Tiessen, P. Geigenberger and N. G. Halford (2006). "Production of high-starch, low-glucose potatoes through over-expression of the metabolic regulator SnRK1." Plant Biotechnology Journal **4**(4): 409-418.

Moretti, J., P. Chastagner, C.-C. Liang, M. A. Cohn, A. Israël and C. Brou (2012). "The Ubiquitin-specific Protease 12 (USP12) Is a Negative Regulator of Notch Signaling Acting on Notch Receptor Trafficking toward Degradation." Journal of Biological Chemistry **287**(35): 29429-29441.

Mosblech, A., C. Thurow, C. Gatz, I. Feussner and I. Heilmann (2011). "Jasmonic acid perception by COI1 involves inositol polyphosphates in Arabidopsis thaliana." The Plant Journal **65**(6): 949-957.

Mulugu, S., W. Bai, P. C. Fridy, R. J. Bastidas, J. C. Otto, D. E. Dollins, T. A. Haystead, A. A. Ribeiro and J. D. York (2007). "A Conserved Family of Enzymes That Phosphorylate Inositol Hexakisphosphate." Science **316**(5821): 106-109.

Munnik, T., R. F. Irvine and A. Musgrave (1998). "Phospholipid signalling in plants." Biochimica et Biophysica Acta (BBA) - Lipids and Lipid Metabolism **1389**(3): 222-272.

Munnik, T. and J. E. M. Vermeer (2010). "Osmotic stress-induced phosphoinositide and inositol phosphate signalling in plants." Plant, Cell & Environment **33**(4): 655-669.

Nijman, S. M. B., T. T. Huang, A. M. G. Dirac, T. R. Brummelkamp, R. M. Kerkhoven, A. D. D'Andrea and R. Bernards (2005). "The Deubiquitinating Enzyme USP1 Regulates the Fanconi Anemia Pathway." Molecular Cell **17**(3): 331-339.

Park, J., B.-S. Lee, J.-K. Choi, R. E. Means, J. Choe and J. U. Jung (2002). "Herpesviral Protein Targets a Cellular WD Repeat Endosomal Protein to Downregulate T Lymphocyte Receptor Expression." Immunity **17**(2): 221-233.

Parra, G., K. Bradnam, A. B. Rose and I. Korf (2011). "Comparative and functional analysis of intron-mediated enhancement signals reveals conserved features among plants." Nucleic acids research.

Perera, I. Y., C.-Y. Hung, S. Brady, G. K. Muday and W. F. Boss (2006). "A Universal Role for Inositol 1,4,5-Trisphosphate-Mediated Signaling in Plant Gravitropism." Plant Physiology **140**(2): 746-760.

Raboy, V. (1997). "Accumulation and Storage of Phosphate and Minerals." Cellular and Molecular Biology of Plant Seed Development. B. Larkins and I. Vasil, Springer Netherlands. **4:** 441-477.

Saiardi, A., R. Bhandari, A. C. Resnick, A. M. Snowman and S. H. Snyder (2004). "Phosphorylation of Proteins by Inositol Pyrophosphates." Science **306**(5704): 2101-2105.

Shears, S. B., N. A. Gokhale, H. Wang and A. Zaremba (2011). "Diphosphoinositol polyphosphates: What are the mechanisms?" Advances in Enzyme Regulation **51**(1): 13-25.

Shen, W., M. I. Reyes and L. Hanley-Bowdoin (2009). "Arabidopsis Protein Kinases GRIK1 and GRIK2 Specifically Activate SnRK1 by Phosphorylating Its Activation Loop." Plant Physiology **150**(2): 996-1005.

Slocombe, S. P., S. Laurie, L. Bertini, F. Beaudoin, J. R. Dickinson and N. G. Halford (2002). "Identification of SnIP1, a novel protein that interacts with SNF1-related protein kinase (SnRK1)." Plant Molecular Biology **49**(1): 31-44.

Smith, T. F., C. Gaitatzes, K. Saxena and E. J. Neer (1999). "The WD repeat: a common architecture for diverse functions." Trends in Biochemical Sciences **24**(5): 181-185.

Stevenson-Paulik, J., S.-T. Chiou, J. P. Frederick, J. d. Cruz, A. M. Seeds, J. C. Otto and J. D. York (2006). "Inositol phosphate metabolomics: Merging genetic perturbation with modernized radiolabeling methods." Methods **39**(2): 112-121.

Styer, J. C., J. Keddie, J. Spence and G. E. Gillaspy (2004). "Genomic organization and regulation of the LeIMP-1 and LeIMP-2 genes encoding *myo*-inositol monophosphatase in tomato." Gene **326**(0): 35-41.

Sugden, C., R. M. Crawford, N. G. Halford and D. G. Hardie (1999). "Regulation of spinach SNF1-related (SnRK1) kinases by protein kinases and phosphatases is associated with phosphorylation of the T loop and is regulated by 5′-AMP." The Plant Journal **19**(4): 433-439.

Szijgyarto, Z., A. Garedew, C. Azevedo and A. Saiardi (2011). "Influence of Inositol Pyrophosphates on Cellular Energy Dynamics." Science **334**(6057): 802-805.

Tan, X., L. I. A. Calderon-Villalobos, M. Sharon, C. Zheng, C. V. Robinson, M. Estelle and N. Zheng (2007). "Mechanism of auxin perception by the TIR1 ubiquitin ligase." Nature **446**(7136).

Tsui, M. M. and J. D. York (2010). "Roles of inositol phosphates and inositol pyrophosphates in development, cell signaling and nuclear processes." Advances in Enzyme Regulation **50**(1): 324-337.

Wang, Y., W.-H. Lin, X. Chen and H.-W. Xue (2009). "The role of Arabidopsis 5PTase13 in root gravitropism through modulation of vesicle trafficking." Cell Res **19**(10).

Zhang, Y., P. J. Andralojc, S. J. Hey, L. F. Primavesi, M. Specht, J. Koehler, M. A. J. Parry and N. G. Halford (2008). "Arabidopsis sucrose non-fermenting-1-related protein kinase-1 and calcium-dependent protein kinase phosphorylate conserved target sites in ABA response element binding proteins." Annals of Applied Biology **153**(3): 401-409.

Zhang, Y., P. R. Shewry, H. Jones, P. Barcelo, P. A. Lazzeri and N. G. Halford (2001). "Expression of antisense SnRK1 protein kinase sequence causes abnormal pollen development and male sterility in transgenic barley." The Plant Journal **28**(4): 431-441.

Zhong, R. and Z.-H. Ye (2004). "Molecular and Biochemical Characterization of Three WD-Repeat-Domain-containing Inositol Polyphosphate 5-Phosphatases in Arabidopsis thaliana." Plant and Cell Physiology **45**(11): 1720-1728.

APPENDIX A

TABLES

Table 1. Primers

GENE	GENE SPECIFIC PRIMER
eGFPFor	5’ CACCATGGTGAGCAAGGGCGAGG 3’
eGFPRev	5’ CTTGTGGCCGTTTACGTC 3’
VIP1For	5’ CACCTTTCGATTTCCAATTAAAAC 3’
VIP1Rev	5’ CTGAGAAAACCTATAAAGCAAC 3’
VIP2For	5’ CACCCAAGAAGAATTATAAGAG 3’
VIP2Rev	5’ CTGAAAAAACCTAGAAAATC 3’

Table 2. List of genes with their accession numbers

GENE	ACCESSION NUMBER
P80	At3g05090
SnRK1.1	At3g01090
SnRK1.2	At3g29160
5PTase 13	At1g05630
VIP1	At3g01310
VIP2	At5g15070

Table 3. List of Constructs used

GENE	PLASMID NAME	PARENT PLASMID	ANTIBIOTIC RESISTANCE	NAME OF RESEARCHER
SnRK1.1	pSnRK1.1:GFP	pK7FWG2	Kanamycin	Elitsa Ananvieva
SnRK1.2	pSnRK1.2:GFP	pK7FWG2	Kanamycin	Janet Donahue
P80	P80:GFPB	pK7FWG2	Kanamycin	Janet Donahue
VIP1	pVIPInt:GUS	pBGWFS7	BASTA	Padma Rangarajan
VIP2	pVIP2Int:GUS	pBGWFS7	BASTA	Padma Rangarajan